INVESTIGATING THE CAUSE OF UNIQUE MECHANICAL BEHAVIOR IN PLATINUM ALLOY GUIDEWIRE TIPS

A Senior Project

presented to

the Faculty of the Materials Engineering Department

California Polytechnic State University, San Luis Obispo

In Partial Fulfillment

of the Requirements for the Degree

Bachelor of Science

by

Evan Borgeson, Alfred Rosen

June, 2015

Abstract

Evan Borgeson, Alfred Rosen, Prof. Blair London (Cal Poly), Abbott Vascular (Temecula, CA)

The platinum alloy used by Abbott Vascular in guidewire tips exhibits a yielding behavior characterized by an abrupt transition from elastic to plastic zones and high ductility. This yielding behavior was hypothesized to be a result of one of three structural phenomena: ordering, solute strain aging, or interstitial strain aging. To test for these strengthening mechanisms in the wire, X-ray diffraction analysis, heat treatments, and tensile testing were completed. The wire has a diameter of 0.0025 inches and was supplied in two forms, the final stress relieved state, and as-drawn from the production line. Heat treatments were performed at 130^{o}C, 250^{o}C, 400^{o}C, and 600^{o}C for a period of one hour. Heat treatments were also performed at 250^{o}C for four hours and eight hours. Heat treating in the theoretical ordering range, between 130-400^{o}C, revealed an increased tensile strength of the wire from 1600 MPa to 1800 MPa. Once heat treated outside of the possible ordering region, at 600^{o}C, the wire showed the same characteristics in tension as the stress relieved wire, which could to be due to an annealing and strain aging mechanism. X-ray diffraction was performed using the Siemens D5000 diffractometer to characterize the crystal structure of the wire. XRD revealed an FCC structure corresponding to the platinum 27 at. % nickel lattice constant, with little evidence of ordering. Superlattice reflections, which appear in XRD and indicate ordering, were not detected. This may have been due to sample preparation, or because the wire is highly textured from the manufacturing process of wire-drawing. Although the XRD failed to find evidence of ordering, this does not mean it is not present within the wire. Strain aging may also be present within the wire, but could not be found due to the nature of Cottrell atmospheres and the difficulty of finding interstitial atoms without proper equipment.

Keywords: Platinum, Ordering, Strain Aging, Cottrell Atmospheres, Guidewires, Medical Devices, Precious Metal, Materials Engineering

Acknowledgments

We would like to thank our project advisor Prof. Blair London for his support and guidance throughout the entire project. We would also like to thank the entire Materials Engineering faculty and staff for their willingness to lend a hand when asked. Lastly, we would like to thank John Simpson at Abbott Vascular for his expertise, and for sponsoring this project, providing samples and testing fixtures, and his thought-provoking questions.

TABLE OF CONTENTS

Introduction **1**
Project Overview 1
Company Background 1
Device Background 2
Pt/Ni Guidewire Application 4
Yielding Properties of Pt/Ni 5
Ordering 5
Yielding Behavior and Ordering 7
Ordering in Pt/Ni 9
Detection of Ordering 11
Strain Aging 13
Cottrell Atmospheres 13
Pt/Ni Strain Aging 14
Cottrell Atmosphere Detection 14
Problem Statement 15
Experimental Procedure **16**
Safety 16
Heat Treatments 16
Tensile Testing 17
X-ray Diffraction 18
Results **21**
Tensile Testing 21
X-ray Diffraction 27
Discussion **29**
Conclusions **35**
References **36**
Appendix **38**

LIST OF FIGURES

Figure 1: A typical surgical guidewire system in the original packaging sheath.[4] 2
Figure 2: Graphical representation of the trend toward more endovascular surgeries. The graph also indicates a decrease in more drastic surgical techniques such as amputation.[5] 3
Figure 3: Diagram of the Abbott Hi-Torque Balance Middleweight Universal guidewire. The tip coil section of interest is highlighted in red.[6] 3
Figure 4: A guidewire (black) shown within the body which is made visible using fluoroscopy (X-rays).[6] 4
Figure 5: Three tensile tests of Pt/Ni wire done by Abbott. The "+" indicates yielding. The yielding behavior is sharp and the plastic zone is extremely linear giving the curve a squared shape.[6] 5
Figure 6: An FCC ordered unit cell. The Pt is represented by the black atoms and the white represents the Ni. In this case simple cubic superlattices are formed by the nickel.[8] 6
Figure 7: Representation of a disordered phase (a) and an ordered structure (b) with an antiphase boundary marked by the dashed line. 7
Figure 8: Stress-strain curves for ordered and disordered Ni_3Fe showing the yield point and higher strength in the ordered structure.[10] 8
Figure 9: Yield stress as a function of domain size, showing the peak strength around 40Å and a decrease as domain size increases or decreases.[10] 9
Figure 10: The 1986 study into Pt/Ni shows ordering of a Ni_3Pt phase around 25 at% Pt and a NiPt ordered phase around 50 at% Pt. The diagram does not indicate ordering at 75 at% Pt.[11] .. 10
Figure 11: The phase diagram developed in 2009 by Lu indicates an additional $NiPt_3$ phase at 75 at% Pt.[12] 11
Figure 12: Two X-ray diffraction patterns of an Au/Cu system. The diffraction pattern (a) is fully disordered. The pattern (b) is a partially ordered system with superlattice reflections indicated by red lines.[13] 12
Figure 13: An example of superlattices in a selected area diffraction pattern of gold copper. The spots indicated with the arrows are superlattices indicative of ordering.[14] 12
Figure 14: Tensile testing of the same alloy. (A) The sample is removed from the tensile tester for a short time and reloaded. The sample does not show a sharp yield point. (B) The same sample is removed after the same tensile strain but is removed from the tensile tester for a period of months before being retested. The sharp yield point returned and the strength increased.[7] 13
Figure 15: Diagram of an interstitial dislocation atmosphere. This dislocation is marked by the extra plane of red atoms and is pinned by the black interstitial atom. 14
Figure 16: The boat used to house the wires during heat treatment. Since the cold worked wires are curled, the aluminum foil was used to keep the wires from falling out of the boat. 17
Figure 17: A fractured tensile sample. The grips are lined with abrasive paper to prevent wire pull out. 18
Figure 18: X-ray sample prepared by placing wire on double sided tape. In this sample 50 wires were placed side by side to fill an area of 6.35 mm in width. 20
Figure 19: Tensile test data for stress relieved wire. The curves for each sample were consistent and showed high ductility. 21

Figure 20: Cold worked wire mechanical behavior shows a gradual yield to fracture at a higher strength than SR wire. 22
Figure 21: The 130°C heat treated wire shows a similar curve shape and properties to the CW wire. 22
Figure 22: The 250°C 1 hour heat treatment caused the highest strength. The wire showed a linear elastic behavior to fracture. 23
Figure 23: Heat treatments at 250°C with varying time showed little difference when compared to each other. All three times had a similar ductility and strength. 24
Figure 24: The 400°C wire showed a decrease in strength and a decrease in ductility. The curve shape of this treatment is also extremely linear in comparison to the cold worked wire. 24
Figure 25: The 660°C heat treatment showed a return to the stress relieved state, and exhibited almost the exact same yield strength and ductility as the as-received stress relieved wire. 25
Figure 26: Average stress-strain behavior for each sample type. The graph shows the significant change in properties caused by differing heat treatment temperatures. 26
Figure 27: X-ray diffraction pattern of Stress Relieved wire from 38 to 90 2θ. Superlattice reflections are absent and are indicated by the blue lines. The (111) reflection is smaller than expected due to microstructure texture. 27
Figure 28: Cold worked wire diffraction pattern from 38 to 90 2θ. The signal-to-noise ratio was poor, due to difficulties with sample preparation. Superlattice reflection locations are shown by the blue lines. 28
Figure 29: Diffraction pattern from 38 to 90 2θ of a 250°C four hour heat treated wire. Calculated superlattice reflection locations are indicated by blue lines. This scan represents the best signal-to-noise ratio achieved. 29
Figure 30: Heat treatment temperatures shown with their locations on the computer modeled phase diagram. The temperatures within the ordered region showed high strength and the temperature outside showed low strength with high ductility. 32
Figure 31: The boxplot of strength distributions for each sample type. Statistical overlap can be seen in several of the samples. However, a clear difference is seen in some of the heat treated samples. 33

LIST OF TABLES

Table I: Fundamental Lattice Reflections ……18
Table II: Superlattice Reflections ……18
Table III: Average Mechanical Properties of Heat Treated and As-received Wire …… 21

Introduction

Project Overview

This project, sponsored by Abbott Vascular (Temecula, CA), is concerned with the mechanical properties of a platinum alloy used in guidewires. The focus is finding the structural phenomena to explain the observed abrupt yielding of a platinum nickel alloy wire. By understanding the specific structural reason behind the behavior, the company will have the knowledge to make improvements on their existing technologies. The hypothesized structural origins for the yield behavior are ordering of the alloy, or strain aging from interstitial or substitutional elements. The specific phenomena acting in the wire was analyzed using mechanical and X-ray diffraction testing.

Company Background

Abbott Laboratories is a multibillion-dollar, multinational healthcare and pharmaceutical company. It operates in a wide range of markets, including pharmaceuticals, medical devices, diagnostics, nutritional products, and animal health products. The company has reported annual revenue of $39.9 billion, and an annual income of $8.1 billion. It employs approximately 90,000 people in over 130 different countries across the world.[1] Abbott has seven divisions within the company, which are: Animal Health, Diabetes Care, Diagnostics, Molecular, Nutrition, and Vascular. Each division is focused on specific aspects within the company, but is managed by the umbrella structure of Abbott. Abbott Vascular is the division of the company that specializes in cardiovascular research and development of new technology, along with the manufacture of existing intervention devices. The main products that they produce are stents, catheters, guidewires, and angioplasty balloons. The vascular division produces many different varieties of guidewires. While many companies produce this technology, Abbott Vascular one of the largest producers of guidewires in the world. They sell $579 million worth of guidewires annually[2] to be used in endovascular surgery around the world.

Device Background

Medical guidewires are high precision surgical tools used to place stents, catheters, and many other implants into patients through their coronary and peripheral vascular system (Figure 1). Most often these wires are used in intensive neurological and coronary surgery that require intricate operations through extremely small vasculature. Guidewires are placed into the body with a catheter and controlled by a surgeon, who sees the wire with X-rays. The device that is being implanted is threaded onto the guidewire, and the surgeon uses the wire to place the medical device into the body. There are many guidewire types, each specialized to do certain tasks or perform specific functions.[3]

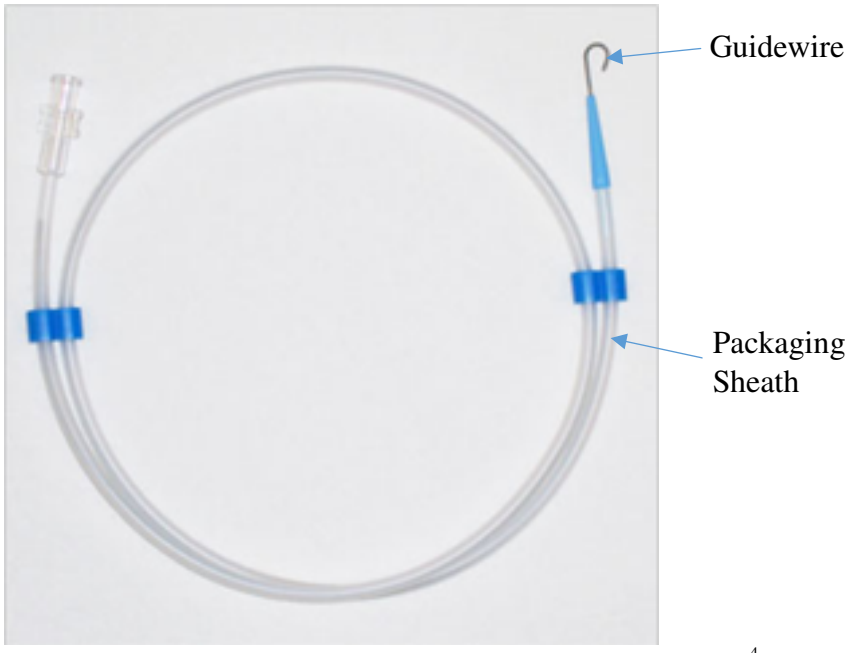

Figure 1: A typical surgical guidewire system in the original packaging sheath.[4]

Guidewire technology is mainly used in minimally invasive endovascular (inside blood vessels) surgeries. These procedures are used to manage diseases within the vascular system, using stents, angioplasty balloons, valve replacements, and other techniques. There are over a million endovascular surgeries performed each year and the use of this surgical technique is growing (Figure 2).[5] Endovascular surgery has been shown to improve the recovery rate of the patient over traditional open vascular techniques. It also improves the success and safety of vascular surgeries.

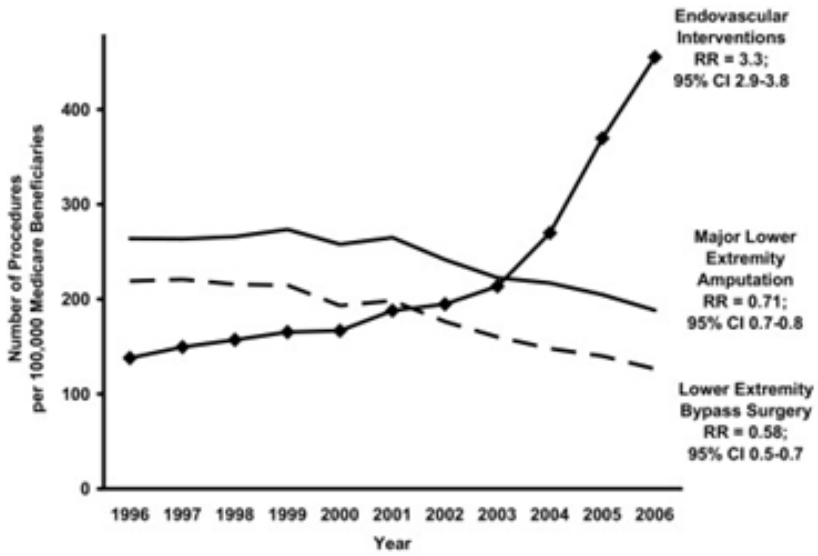

Figure 2: Graphical representation of the trend toward more endovascular surgeries. The graph also indicates a decrease in more drastic surgical techniques such as amputation.[5]

Guidewires are comprised of several parts, each of which serve an individual function. The stainless steel core is the backbone of the entire wire, and what the surgeon grasps when he uses the wire. The core wire is coated with Teflon to make it hydrophobic or hydrophilic, and ground to a taper of 0.002□□ diameter. A stainless steel wire coil is placed around the tapered section of the core, which adds flexibility to the guidewire (Figure 3). The tip of the wire is composed of a radiopaque platinum alloy coil, which allows the wire to be seen under fluoroscopy.[6] The tip coil is soldered to the core wire on both ends, securing it to the wire.

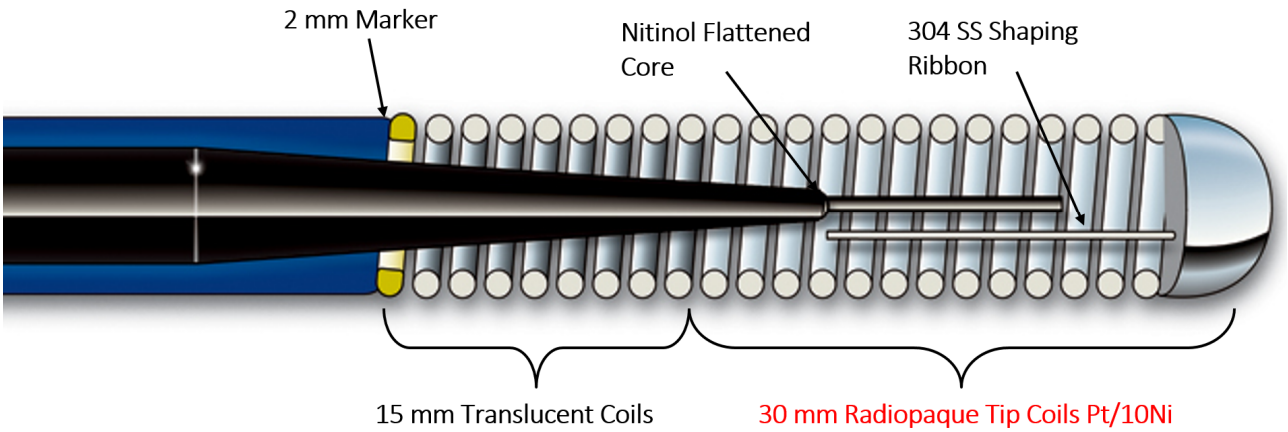

Figure 3: Diagram of the Abbott Hi-Torque Balance Middleweight Universal guidewire. The tip coil section of interest is highlighted in red.[6]

Pt/Ni Guidewire Application

Platinum alloys are often utilized for their unique radiological properties, particularly for being radiopaque under X-ray. Currently, Abbott Vascular uses a platinum nickel alloy wire as a tip coil in many of their guidewires. The tip coil functions as a flexible and formable end to the guidewire that can be seen through fluoroscopy (Figure 4). The operator forms the coil tip into a "J" or "L" shape in order to have better control of artery selection as the guidewire travels through the body. Because of the need for formability, the initial plastic deformation of Pt/Ni is of special concern.[6] The tip coil needs to remain round, and not "pancake" when deformed, so that it can remain fully functional. If the wire coil loses shape when deformed, it may not function properly when in use, which could mean a stent or angioplasty balloon cannot reach the intended implant site. Situations like this can be dangerous for a patient's health and costly to a hospital. For this reason, the guidewire tip needs to be reliable in use for a surgeon.

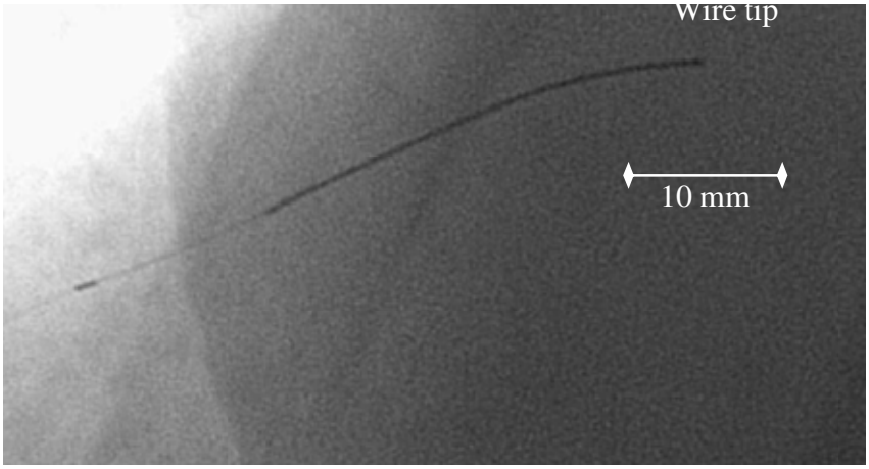

Figure 4: A guidewire (black) shown within the body which is made visible using fluoroscopy (X-rays).[6]

Yielding Properties of Pt/Ni

Pt/Ni yielding behavior is important to the application because the operator of the guidewire plastically deforms the tip core without damaging the Pt/Ni tip coil before it is used in the body. The reason Pt/Ni is preferred over other radiopaque alloys is its sharp yield point and high strength. In tensile testing of wires used by Abbott the material transitions abruptly from elastic deformation to plastic (Figure 5). The transition is atypical of alloys and is the focus of the investigation.

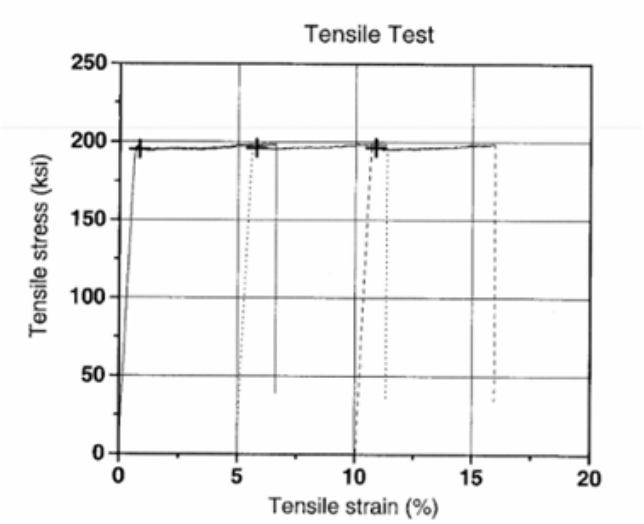

Figure 5: Three tensile tests of Pt/Ni wire done by Abbott. The "+" indicates yielding. The yielding behavior is sharp and the plastic zone is extremely linear giving the curve a squared shape.[6]

The abrupt transition from elastic to plastic behavior of the material is repeatable over all tests and suppliers. Abbott requires their suppliers to stress relieve the wire to achieve specified requirements for straightness, ductility, and strength. In order to achieve the desired properties, the supplier heat-treats the wire after wire drawing. The heat treatment is proprietary and unknown. However, it is hypothesized that it may trigger a strengthening mechanism. These mechanisms include ordering and strain aging. It is also possible that these mechanisms could occur independently of the heat treatment.

Ordering

Ordering is the formation of a crystal structure where each alloying element occupies a specific lattice position. Ordering in alloys occurs at specific compositions such as 50/50 at% and 75/25

at%. The effect of ordering is the formation of superlattices. A superlattice occurs when individual alloying elements occupy specific lattice locations. Ordered systems occur due to lower energy states that prefer A-B atomic interactions to A-A or B-B. For example, in the case of Au/Ni system, when the system is fully disordered the fit between atoms is poor and the lattice is strained. The lattice can achieve a lower strain energy by forming an ordered arrangement. There is less strain when the gold and nickel atoms arrange into alternating or superlattice structures.[7] The degree of ordering is variable due to non-exact compositions and imperfect crystal structures. In the case of the Pt/Ni being studied the atomic percentage is 73% Pt and 27% Ni. This corresponds well with a Pt_3Ni ordered structure (Figure 6). However, it is unknown whether this ordered phase exists in the Abbott wire.

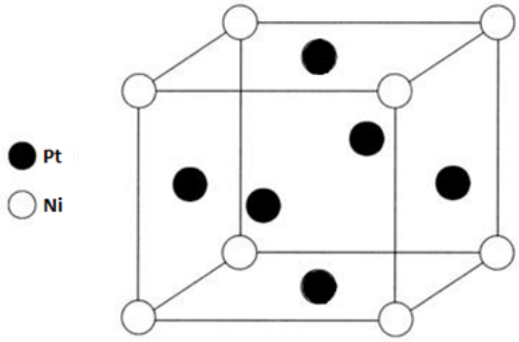

Figure 6: An FCC ordered unit cell. The Pt is represented by the black atoms and the white represents the Ni. In this case simple cubic superlattices are formed by the nickel.[8]

Ordered alloys contain domains, which are areas of order that do not match up with each other, similar to grains in polycrystalline materials. An antiphase domain is a group of ordered atoms that are configured opposite to the majority of other ordered atoms in the material (Figure 7). Between these antiphase domains and the parent domain there are boundaries, called antiphase boundaries. These boundaries are areas of disorder between the ordered structures, similar to a grain boundary. Within a single ordered grain there are many domains. More ordered structures contain fewer, larger domains, while less ordered structures have more, smaller domains. Antiphase boundaries can easily be seen in thin films using a transmission electron microscope.[9]

Disordered Ordered

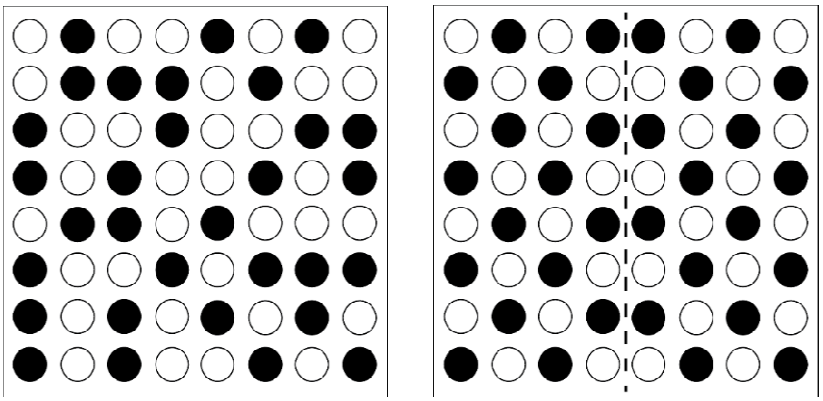

(a) (b)

Figure 7: Representation of a disordered phase (a) and an ordered structure (b) with an antiphase boundary marked by the dashed line.

Yielding Behavior and Ordering

Alloys that show long range order have been shown to work-harden more rapidly than alloys that are disordered. This phenomenon can be explained by a few theories, the first of which proposes that as the ordered alloy is deformed the domain size decreases. The decreasing domain size causes increased stress to be needed to produce the same strain. This theory asserts that the work hardening behavior of the alloy is domain size dependent. Another theory postulates that the work hardening is largely independent of domain size, but actually due to antiphase domains left behind by jogged superdislocations moving through the structure. Superdislocations are perfect dislocations of the superlattice, which are separated by an antiphase boundary. The increase in energy required to drag jogs through the lattice appears as an increase in the work hardening of the alloy. Both of these theories are based on the formation of antiphase boundaries to increase strength.[10]

Ordered alloys exhibit a sharp yield point in addition to having a higher yield strength and higher tensile strength when compared to their disordered counterparts (Figure 8). The sharp yield point can be explained by the changing domain sizes and the antiphase boundary widths as the alloy is strained. The behavior can be explained by Cottrell's formula:

(Equation 1)

Where = the observed yield point

= a numerical factor, depending on the shape of the domains

= the antiphase boundary width

= the domain size

= the antiphase boundary energy

This shows the yield point's dependence on the domain size and antiphase boundary width. Once the yield point is reached, there are a significant amount of dislocations moving through the structure, forming more domains and antiphase boundaries. The smaller domain sizes causes a slight decrease in strength which can be seen as the yield point (Figure 9).[10]

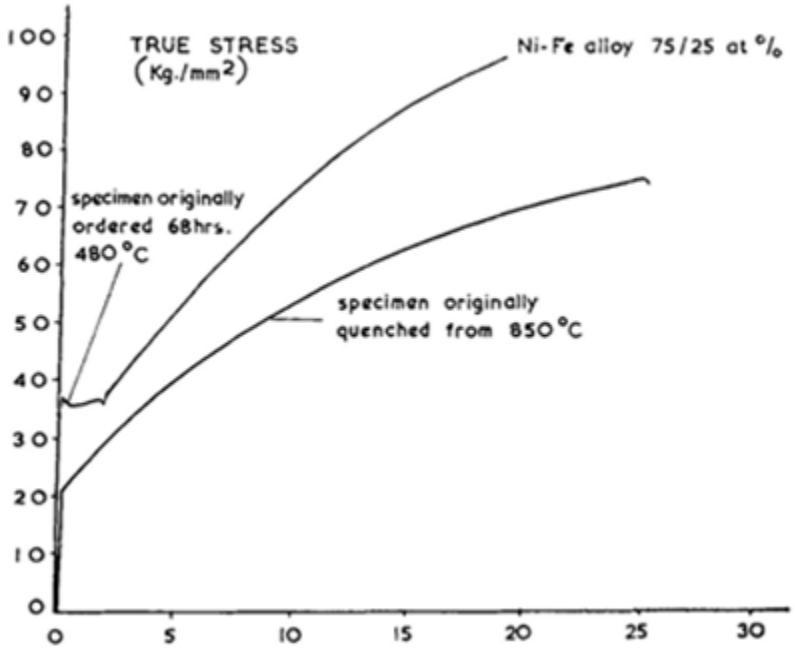

Figure 8: Stress-strain curves for ordered and disordered Ni_3Fe showing the yield point and higher strength in the ordered structure.[10]

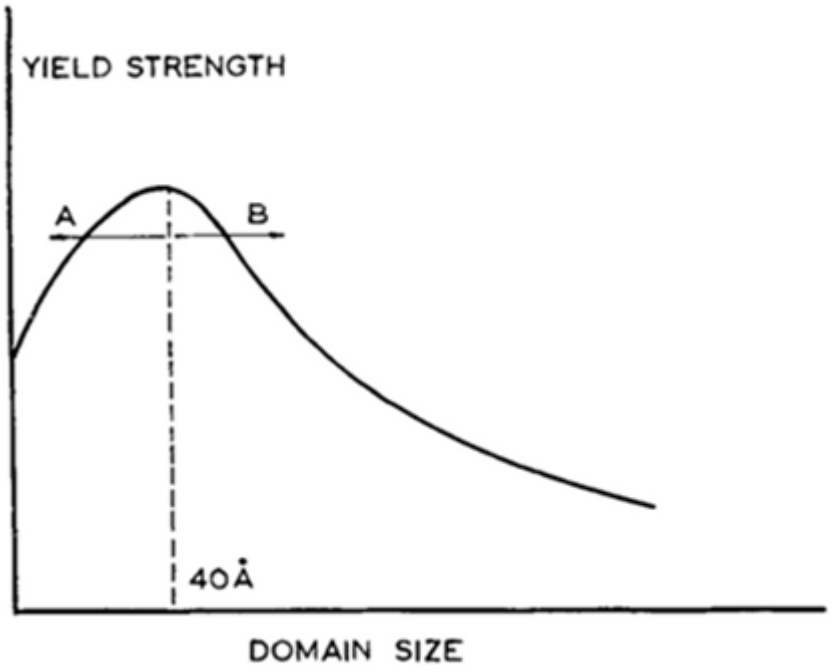

Figure 9: Yield stress as a function of domain size, showing the peak strength around 40Å and a decrease as domain size increases or decreases.[10]

Ordering in Pt/Ni

The thermodynamics of the Pt/Ni system suggest a number of different ordered phases may occur at various compositions. In 1986 the structure of Pt/Ni was analyzed and shown to only contain a small amount of ordering and have mostly a solid solution structure (Figure 10). At 73 at% Pt no ordering is indicated by the study. If the phase diagram proves to be accurate, it would disprove the hypothesis of the effects of ordering causing strengthening and influencing yielding behavior in the Abbott wire. If ordering is disproven, then a different strengthening mechanism is present in the guidewire material.[11]

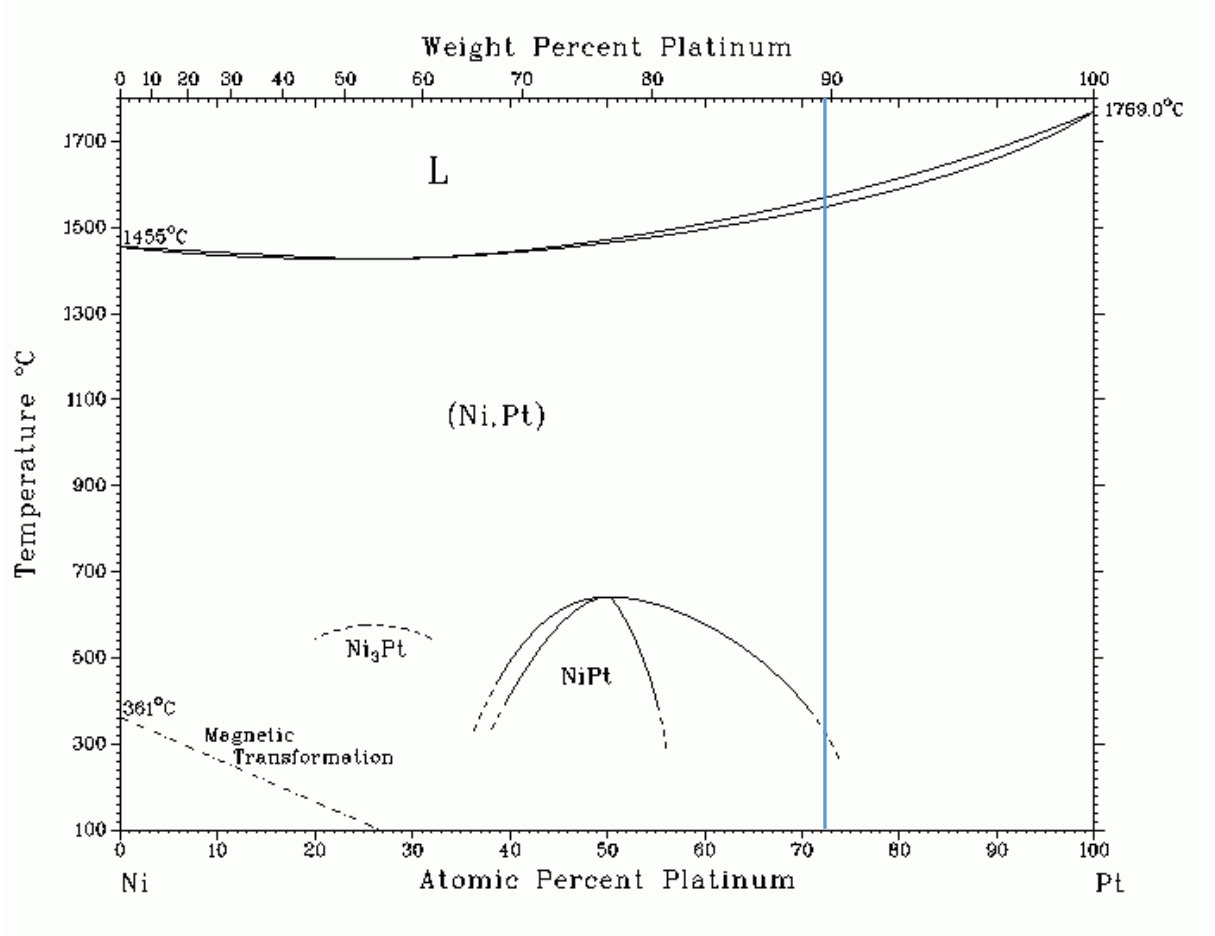

Figure 10: The 1986 study into Pt/Ni shows ordering of a Ni_3Pt phase around 25 at% Pt and a NiPt ordered phase around 50 at% Pt. The diagram does not indicate ordering at 75 at% Pt.[11]

A 2009 study by Xiao-Gang Lu into the thermodynamics of the Pt/Ni system revealed that four different solid phases occur and indicates that the 1986 Nash study may have missed some phase ordering. At high temperatures the system is a complete solid solution. However, at lower temperature three ordered phases are revealed including Ni_3Pt and NiPt which are indicated by Nash in Figure 6 but also a $NiPt_3$ phase at about 75 at% Pt or around 90 wt% Pt (Figure 11). The phase diagram was developed using CALPHAD software modeling. The theoretical existence of the ordered phases suggests that the yielding behavior of the Abbott wire could be explained by ordering but the model does not necessarily prove the phase's existence in actual experimentation.[12]

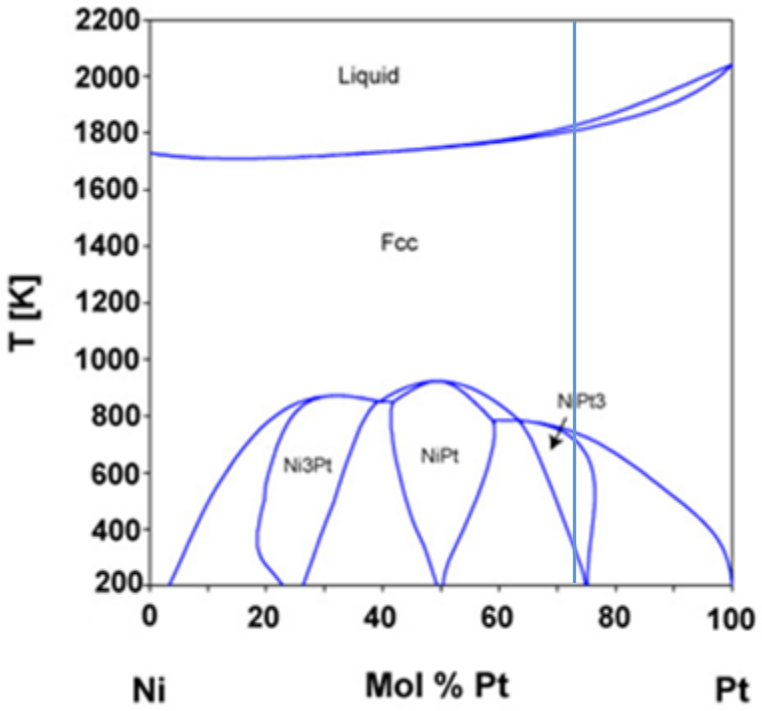

Figure 11: The phase diagram developed in 2009 by Lu indicates an additional $NiPt_3$ phase at 75 at% Pt.[12]

Detection of Ordering

X-ray diffraction (XRD) is a tool used to probe the crystal structure of materials. A beam of X-rays is diffracted off the material and is reflected in many directions. By measuring the angles and the intensity of the X-rays being reflected the crystal structure can be analyzed. A diffraction pattern that shows the intensity of reflection over the angle of the beam indicates when a crystallographic plane reflects X-rays. The angle of the reflection is indicative of a specific plane of interaction so by reading the diffraction pattern the crystal structure can be found.[13]

XRD is useful for analyzing an alloy for long range order. The diffraction pattern will show reflections indicative of the overall crystal structure but will also reveal superlattice reflections that are a result of the secondary crystal structure from individual alloying elements in ordered structures (Figure 12). The superlattice reflections are of less intensity than the fundamental reflections because of destructive interference caused by the two element's competing secondary crystal structure.[13]

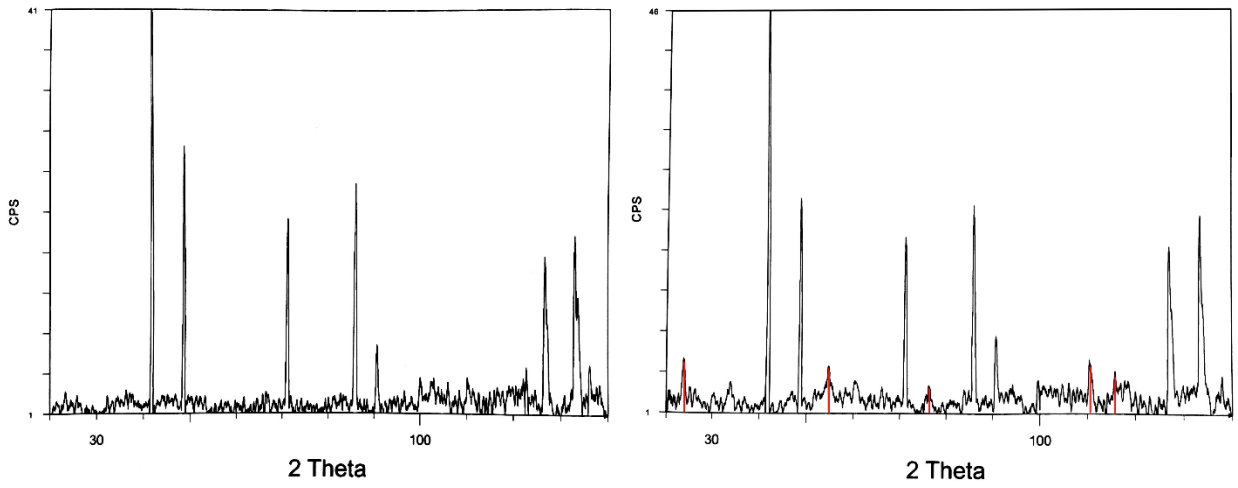

(a) (b)

Figure 12: Two X-ray diffraction patterns of an Au/Cu system. The diffraction pattern (a) is fully disordered. The pattern (b) is a partially ordered system with superlattice reflections indicated by red lines.[13]

Another method used for detection of ordering is selected area electron diffraction (SAD). SAD is a technique that uses a transmission electron microscope (TEM) where electrons (treated as waves) are transmitted through a material. The material's crystal structure acts as a diffraction grating and spreads the electron beam. The resulting diffraction pattern reveals characteristics of the crystal structure as the angles of the diffraction spots. Superlattice diffraction patterns occur within the lattice and are visible as smaller secondary spots (Figure 13).[14]

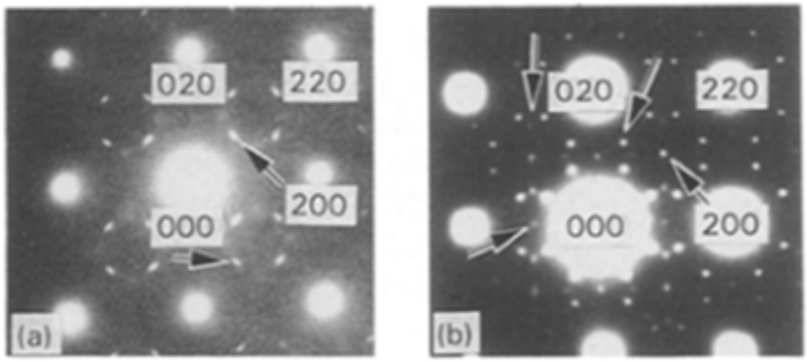

Figure 13: An example of superlattices in a selected area diffraction pattern of gold copper. The spots indicated with the arrows are superlattices indicative of ordering.[14]

The SAD method of detecting superlattices is similar to that of XRD but can more easily detect ordering when a material is not fully ordered. However, the method only uses a small area of the sample so the superlattice diffraction pattern may only indicate short range and not long range order.[14]

Strain Aging

Strain aging is a phenomenon that occurs in alloys that have been plastically deformed under their tensile strength, unloaded and left to rest. When the material is reloaded immediately after the initial yielding the sharp yield point will not be present. However, if a strain aged sample is reloaded a significant amount of time after deformation, it will have a sharp yield point, much higher than the original (Figure 14). The mechanism for this behavior is theorized to be due to the formation of Cottrell atmospheres around dislocations in the material.[7]

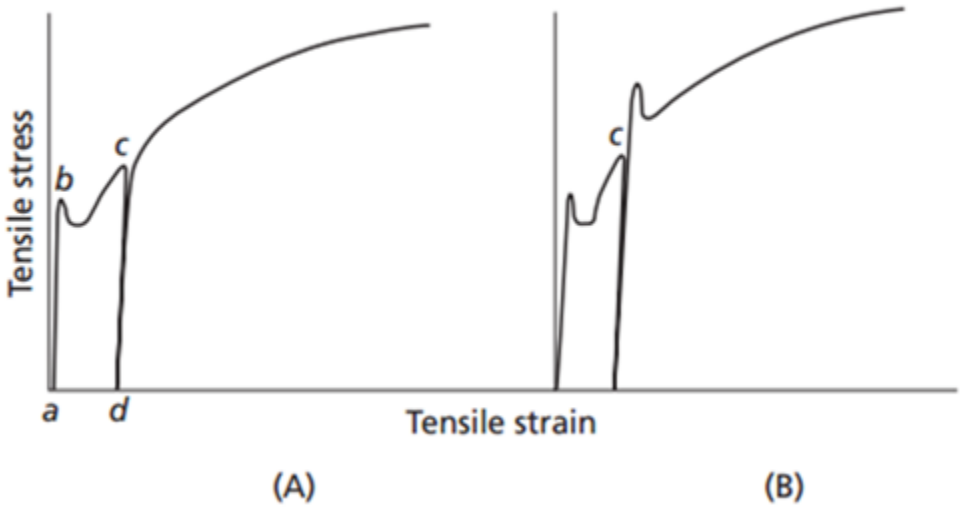

Figure 14: Tensile testing of the same alloy. (A) The sample is removed from the tensile tester for a short time and reloaded. The sample does not show a sharp yield point. (B) The same sample is removed after the same tensile strain but is removed from the tensile tester for a period of months before being retested. The sharp yield point returned and the strength increased.[7]

Cottrell Atmospheres

Strain aging is caused by the movement of solute atoms to dislocation sites to reduce strain fields around the dislocation. After dislocations have been introduced by plastic deformation of the material, the solute atoms move to lock the dislocations in place. The movement of solute atoms occurs through diffusion in the structure. Interstitial atoms, which have higher diffusivity, are able to move through the lattice to form atmospheres (Figure 15). Substitutional atoms usually require elevated temperatures to diffuse through the structure in a reasonable amount of time. The diffusion of solute atoms is time dependent, so the reappearance of the yield point is a function of time.[7]

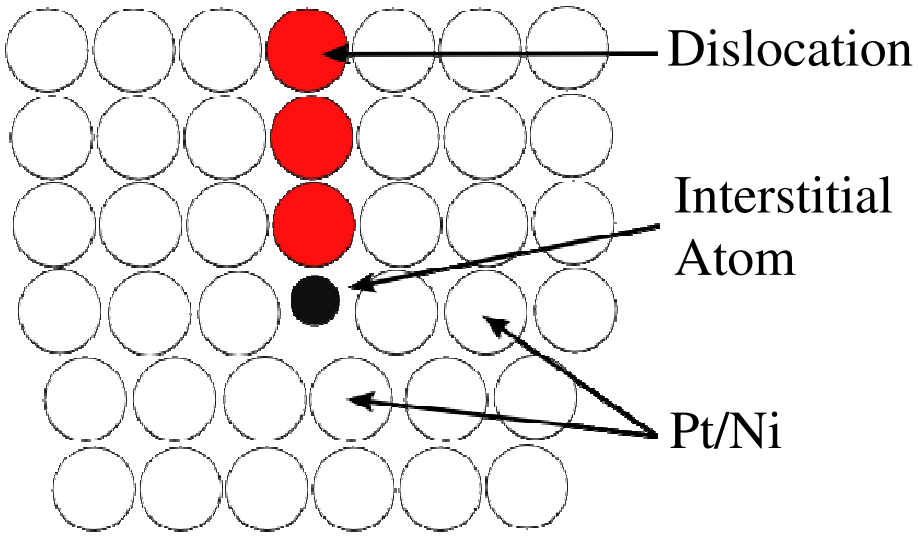

Figure 15: Diagram of an interstitial dislocation atmosphere. This dislocation is marked by the extra plane of red atoms and is pinned by the black interstitial atom.

The mechanism that allows for the sharp yield point is due to an interaction between dislocations and solute atoms in the lattice. The solute atoms collect around dislocations, anchoring them in place and strengthening the alloy. Additional stress is required in order to move the dislocation from the atmosphere, which corresponds to an increase in yield strength. Once the dislocations break free of the atmospheres they can move through the alloy, explaining the drop in strength after yielding.[7]

Pt/Ni Strain Aging

The Pt/Ni tensile tests show a sharp yield point similar to that of strain aging alloys (Figure 5). It is possible that the reason for the abrupt yield is due to the formation of Cottrell atmospheres. The atmospheres may result from an unknown interstitial in the lattice such as oxygen or nitrogen. Atmospheres could also be a result of the supplier's heat treatment to the wire after wire drawing. In the heat treatment either the Pt or Ni atoms could act as substitutional atoms and move toward dislocations to cause atmospheres to form.[15]

Cottrell Atmosphere Detection

Cottrell atmospheres are traditionally difficult to detect but can be inferred from the return of a yield point after a sufficient aging period as illustrated in Figure 10. However, the atmospheres can be observed directly by first identifying a dislocation position by field ion microscopy (FIM) using TEM. Once a dislocation is located, three-dimensional atom probe (3DAP) analysis, which utilizes a position sensitive detector and charge-to-mass ratios to determine the locations of atoms in 3D space, is performed to map the interstitial elements in the region surrounding the dislocation. An increased distribution of interstitials is observed within the atmosphere surrounding the dislocation.[16]

Problem Statement

Guidewire technology utilizes radiopaque platinum nickel alloys. The alloy used by Abbott Vascular in guidewire tips exhibits a sharp yielding behavior characterized by an abrupt yield point and a stress-strain plateau. The structural cause for this material behavior is unknown, and will be addressed by this project. Based on literature, the yielding behavior is hypothesized to be a result of one of three structural phenomena: ordering reaction, solute strain aging, or interstitial strain aging.

In the case of an ordering reaction Pt/Ni forms a Pt_3Ni ordered phase during a heat treatment performed by the supplier post wire draw. The combination of increased bond energies and resistance to superdislocations or jogs results in a sharp yield point. X-ray diffraction testing will reveal superlattice reflections that indicate ordering.

Strain aging is caused by the diffusion of atoms to dislocation sites in the structure, which induce atmospheres that inhibit dislocation movement and is a probable cause for a sharp yield point. Solute Cottrell atmospheres are formed when Ni or Pt atoms form atmospheres around dislocations during the supplier heat treatment. Interstitial Cottrell atmospheres are formed when an unknown interstitial element collects at dislocation sites throughout the alloy. Atmospheres may occur by natural aging or artificial aging during the heat treatment.

Tensile testing and X-ray diffraction were conducted on heat treated and non-heat treated samples to analyze the mechanical behavior for the presence of atmospheres or ordering. The goal of this project was to determine the structural reason for the yielding behavior of the Pt/Ni alloy used by Abbott Vascular.

Experimental Procedure

Safety

Testing for this project included heat treatments, tensile testing, and X-ray diffraction. Safety precautions were taken during each step of the process. General lab safety procedures were followed during the entire project, which included wearing pants and closed toe shoes. When operating furnaces to heat treat the wire, gloves and a face shield were worn. Safety glasses were worn during tensile testing. Radiation exposure was measured and tracked using dosimeters during X-ray diffraction testing.

Heat Treatments

The wire was given to the team in two forms, final stress relieved (SR), and as-drawn cold worked (CW). The cold worked wire was heat treated at 130^{o}C, 250^{o}C, 400^{o}C, and 600^{o}C for one hour. The wire was also heat treated at 250^{o}C for four hours and eight hours. The bottom three temperatures were chosen to be within the theoretical Pt_3Ni ordered range. The upper temperature was chosen to exceed the ordered range of temperatures. This was done to find out more about the effects of elevated temperatures on the wire, and if a different behavior would be observed outside of the ordered region. A Fisher Science high temperature furnace, and a low temperature oven were used to heat treat the wire. The wire was cut into five 70 mm long sections which were each placed into a ceramic heat treatment "boat" (Figure 16). This was done to keep wires from being lost in the furnace, and to handle them better. The boat was wrapped in aluminum foil, to hold the wires in, and placed inside of the furnace. After the heat treatment time was completed for each set of wires, the boat was removed using gloves. The foil

was quickly unwrapped, and the wires laid on the table to air cool. Each treatment of wires was then placed in a separate bag for later testing and evaluation.

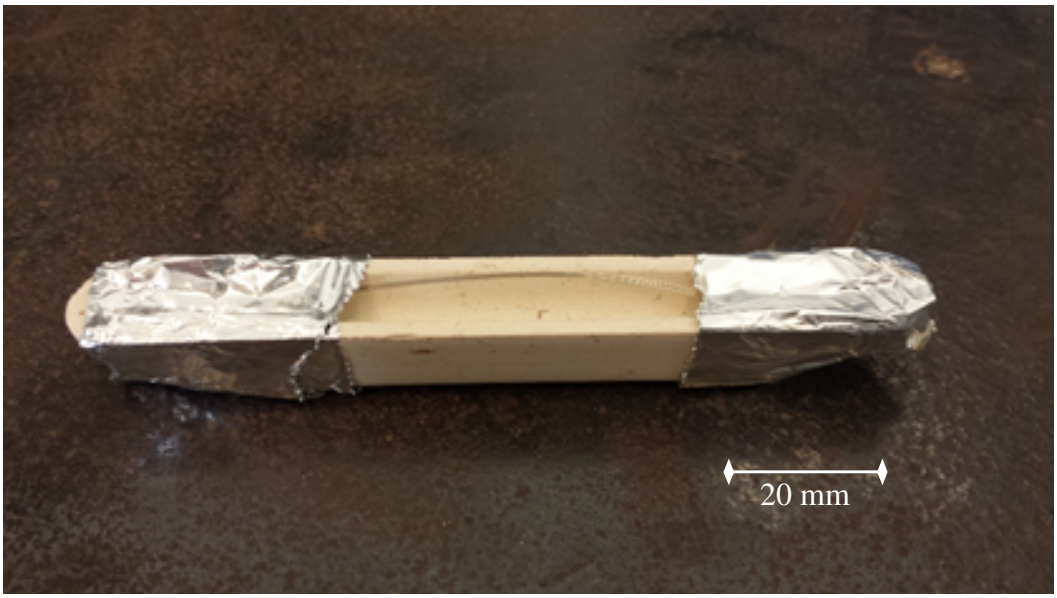

Figure 16: The boat used to house the wires during heat treatment. Since the cold worked wires are curled, the aluminum foil was used to keep the wires from falling out of the boat.

Tensile Testing

Tensile testing produces load and extension data that is used to calculate stress and strain given a sample diameter and gauge length. The gauge length was set at 50mm and a consistent diameter of 0.0635 mm (0.0025 in) was used for all tests. Wire was mechanically tested using a Mini 55 Instron tensile tester, with a 50 N static load cell. The wire was secured with static tensile grips, which were lined with abrasive paper to prevent the wire from slipping (Figure 17). In some cases, additional gripping strength was needed to prevent wire pull-out from the grips, so clamps were attached to the exterior of the grips. The load was balanced prior to specimen loading in order to prevent pre-loading. Slack was removed from the grips to eliminate negative loads after fracture. The cross head speed was set to 1 mm/min to allow for accurate data measurement, and to prevent any chance of pull out in the grips. Due to the size of the samples, and availability of a visual extensometer, crosshead displacement was used to calculate strain.

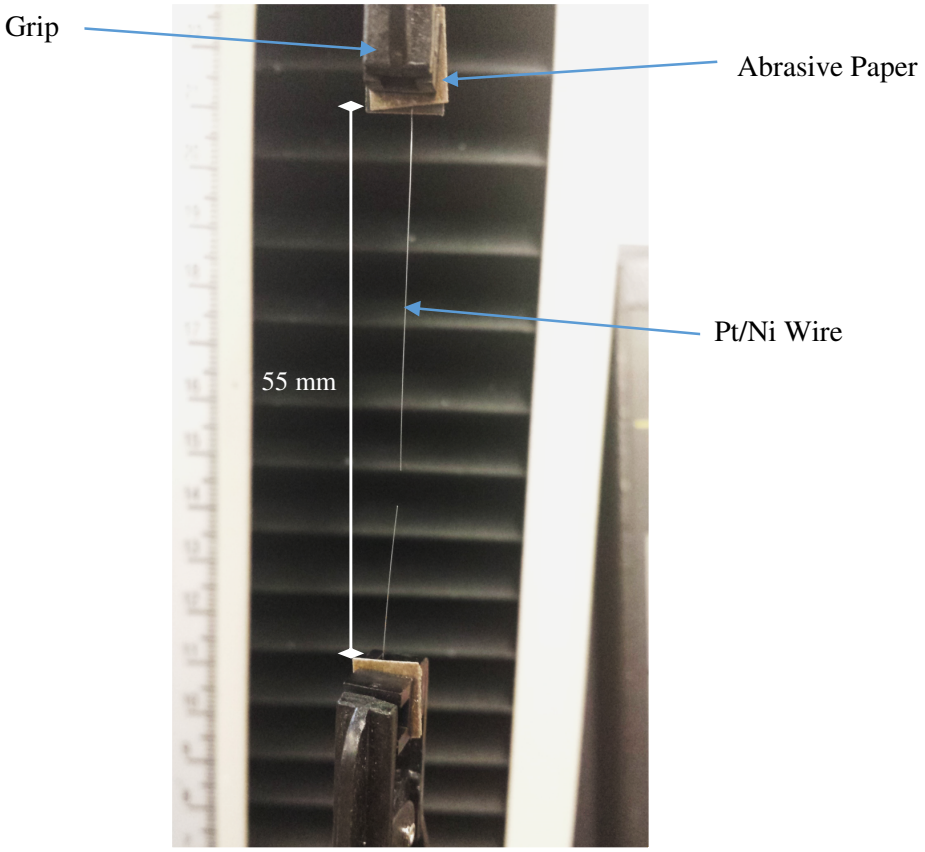

Figure 17: A fractured tensile sample. The grips are lined with abrasive paper to prevent wire pull out.

The data provided by tensile testing was analyzed using the raw data in Excel. Each curve's linear elastic portion was fitted with a trendline. The slope of the line generated is the approximate elastic modulus of the material calculated using crosshead extension. To find yield strength, a line parallel to the elastic trendline was plotted at 0.2% strain and the intersection to the stress-strain curve was found. In some cases the wire fractured before the line could intersect and the maximum stress was used as yield strength. The yield strengths and curve shapes were compared to draw conclusions about the structure and behavior of the alloy system.

X-ray Diffraction

X-ray diffraction was used to try to detect ordering within the wires. The diffraction pattern shows reflections indicative of the overall crystal structure but when ordering is present, it will also reveal superlattice reflections. X-ray diffraction testing was performed on stress relieved, cold worked, and 250^{o}C heat treated wire. The lattice constant was calculated to be 3.8118 Å and

the wavelength was 1.5418 nm. Using these values and Bragg's Law, 2θ locations for the fundamental reflections were determined, found in Table I. Superlattice reflection locations, found in Table II, were also calculated using the same method.

Table I: Fundamental Lattice Reflections in Pt/Ni

hkl	111	200	220	311	222	400	331	420	422
2θ	41.0	47.7	69.8	84.3	88.9	108.0	123.7	129.5	164.4

Table II: Calculated Superlattice Reflection in Pt/Ni

hkl	100	110	210	211	300	310	320	321	410	411	421	332
2θ	23.3	33.2	53.7	59.3	74.4	79.4	93.6	98.3	112.9	118.1	135.7	142.9

The diffractometer was fitted with 1mm divergence and antiscatter slits and a .2mm detector slit. Large scans were performed from 35 to 80 2θ at a scanspeed of 1 degrees per minute and increment of 0.05 degrees. Higher resolution scans were also used at calculated superlattice reflection sites to determine if ordering was present and detectable in the wire. High resolution scans were run at a scanspeed of 0.1 degrees per minute and an increment of 0.01 degrees.

The ideal X-ray diffraction sample is a flat surface, or fine powder. Several different sample preparation methods were used to emulate standard diffraction samples. The most ideal samples had the highest signal-to-noise ratio. A pseudo powder sample was made by cutting the wire into as fine of a size as possible, and placing the pieces into a powder sample tray. The advantage of a powder sample is that grain orientation is randomized. However, the wire could not be fully powderized and sample preparation was not ideal. Samples were also prepared by aligning many wires on a flat glass surface using tape to hold the wire in place. This was done to make the slide as flat as possible, to be an ideal diffraction surface. In some cases wire was bundled and taped at the ends of the sample holder, which caused some of the wire to raise off of the holder's surface. More ideal samples were prepared using double sided tape and carefully aligning wire on the surface of the tape (Figure 18). This type of sample preparation yielded a superior signal-to-noise ratio.

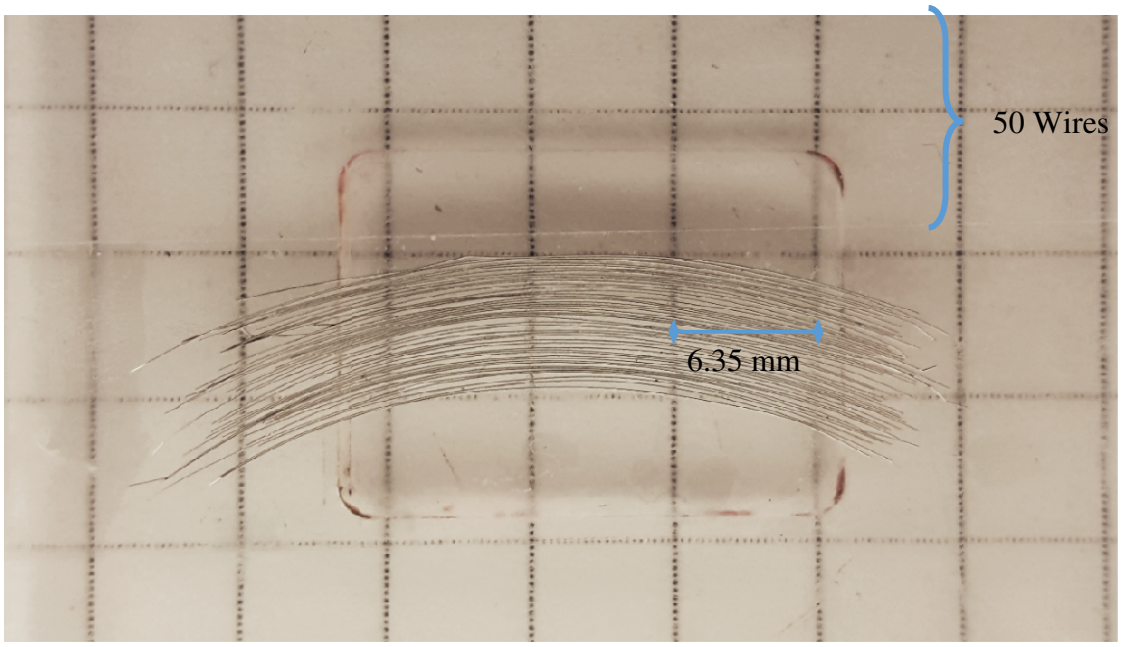

Figure 18: X-ray sample prepared by placing wire on double sided tape. In this sample 50 wires were placed side by side to fill an area of 6.35 mm in width.

X-ray data was qualitatively analyzed for peaks at expected locations using diffraction pattern evaluation software (Bruker EVA). The software was able to eliminate some noise, and boost the signal-to-noise ratio. It also allowed for the data to be viewed in other formats other than the raw data. This data was used to draw conclusions about the presence of ordering and other strengthening mechanisms in the samples.

Results

Tensile Testing

The stress relieved (SR) wire showed a linear elastic response until an abrupt yield around 1250 MPa at which point it showed an almost perfectly plastic response (Figure 19). The wire showed an average ductility of 6.89% and had an ultimate tensile strength of 1300 MPa. The data showed a low standard deviation and was easily replicable.

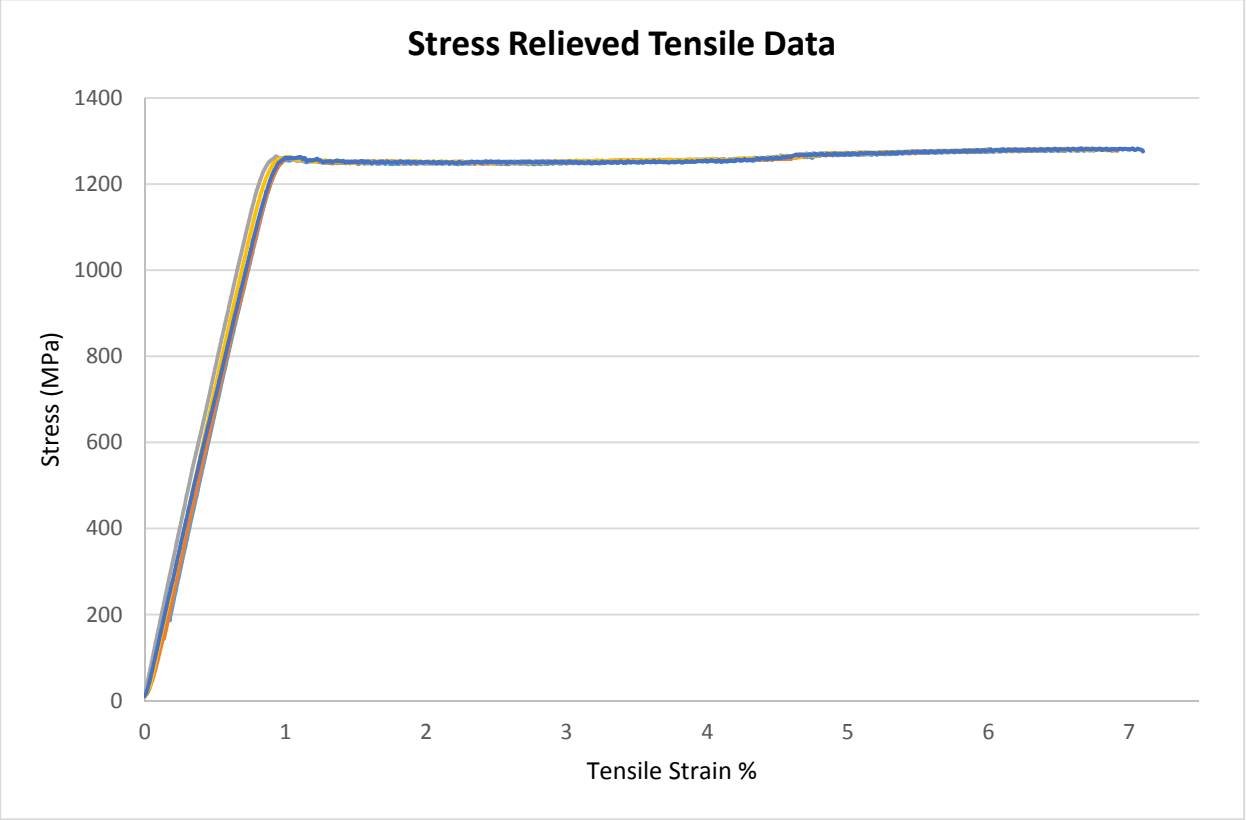

Figure 19: Tensile test data for stress relieved wire. The curves for each sample were consistent and showed high ductility.

The cold worked (CW) wire showed a significant change in strength and ductility from the SR wire (Figure 20). The wire had an average yield strength of 1600 MPa and a percent elongation of 1.43%. The curve has a gradual shoulder to yield unlike the SR wire.

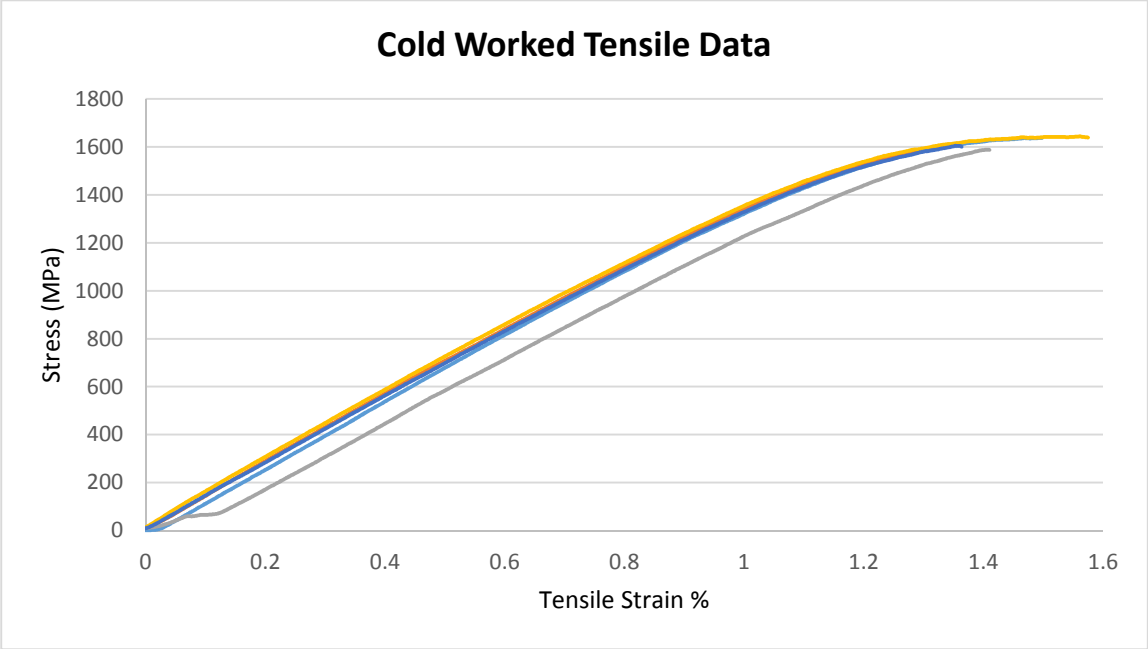

Figure 20: Cold worked wire mechanical behavior shows a gradual yield to fracture at a higher strength than SR wire.

The 130°C heat treatment caused almost no change in strength or ductility compared to the CW wire (Figure 21). It had an average yield strength of 1587 MPa and an average ductility of 1.40% strain. The wire had some distribution in ductility with a range of 1.21% to 1.50%.

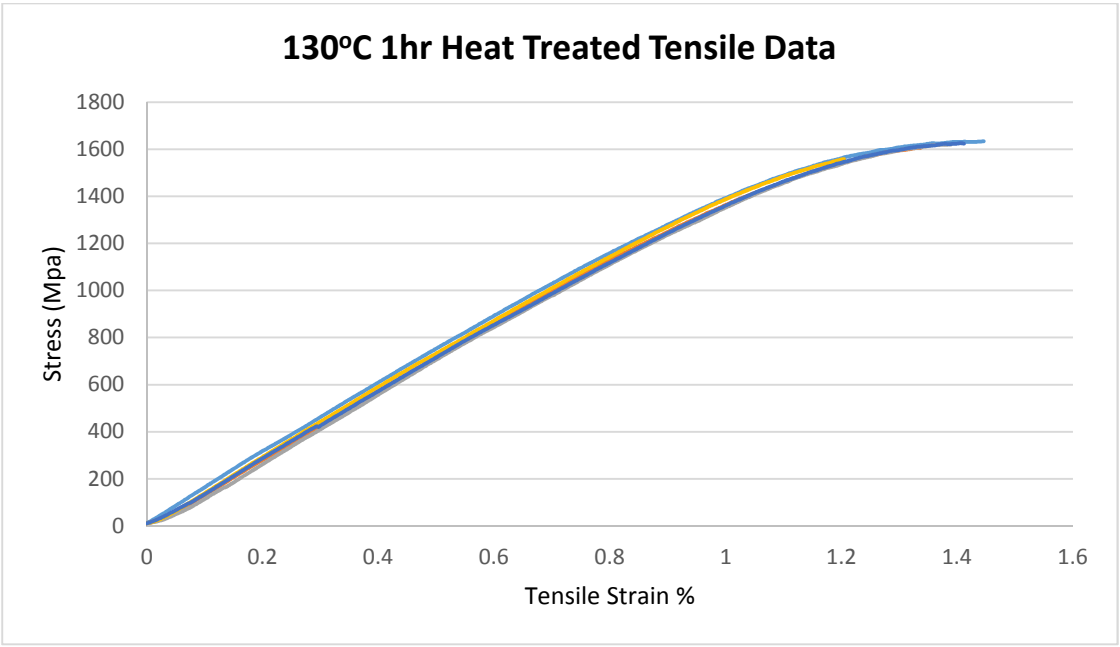

Figure 21: The 130°C heat treated wire shows a similar curve shape and properties to the CW wire.

250°C heat treatments had little variation between heat treatment times but showed a significant increase in strength. The percent elongation remained the same at 1.39%. The sample fractured too suddenly for a 0.2% offset to be used to calculate yield strength so the ultimate tensile strength was used for yield strength. The average yield strength for the wire treated for one hour was the highest of all the tests at 1829 MPa (Figure 22). The four hour samples fractured at an average of 1763 MPa and the eight hour samples fractured at an average of 1784 MPa (Figure 23).

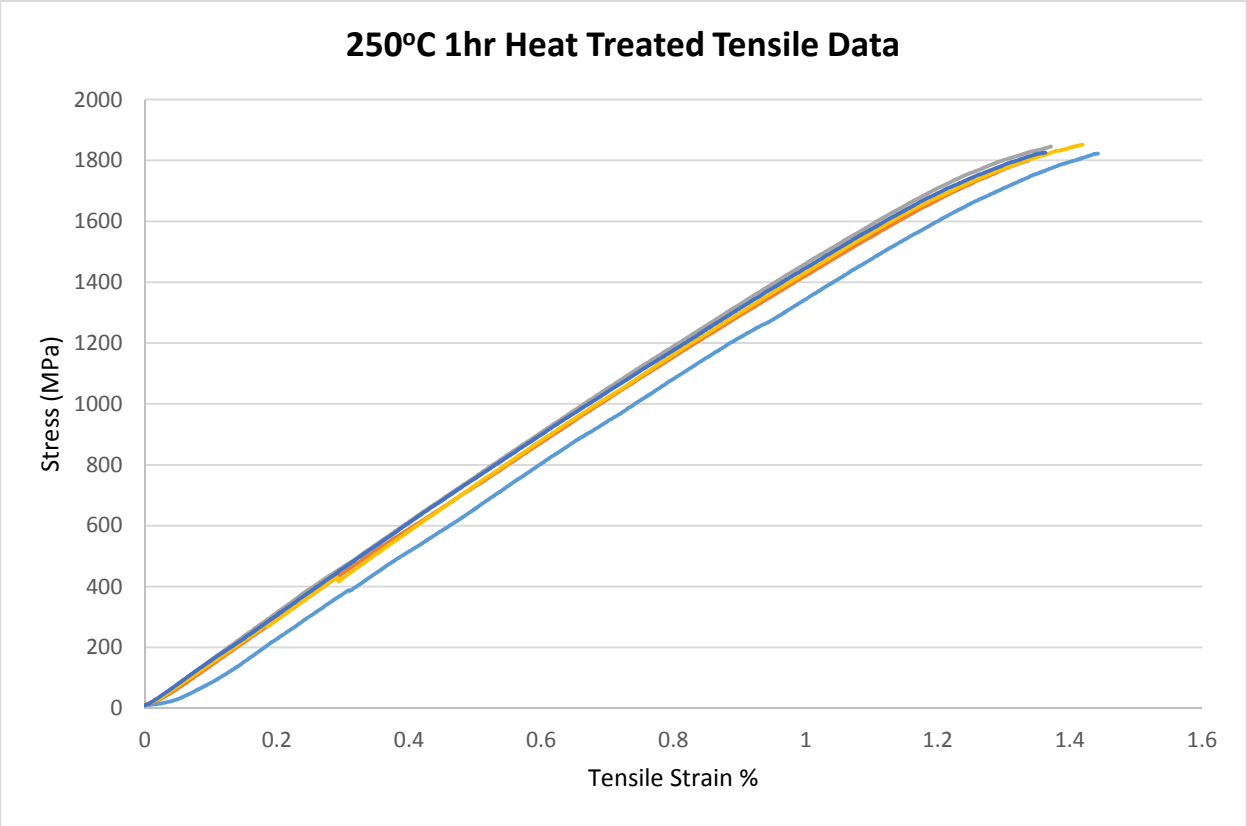

Figure 22: The 250°C 1 hour heat treatment caused the highest strength. The wire showed a linear elastic behavior to fracture.

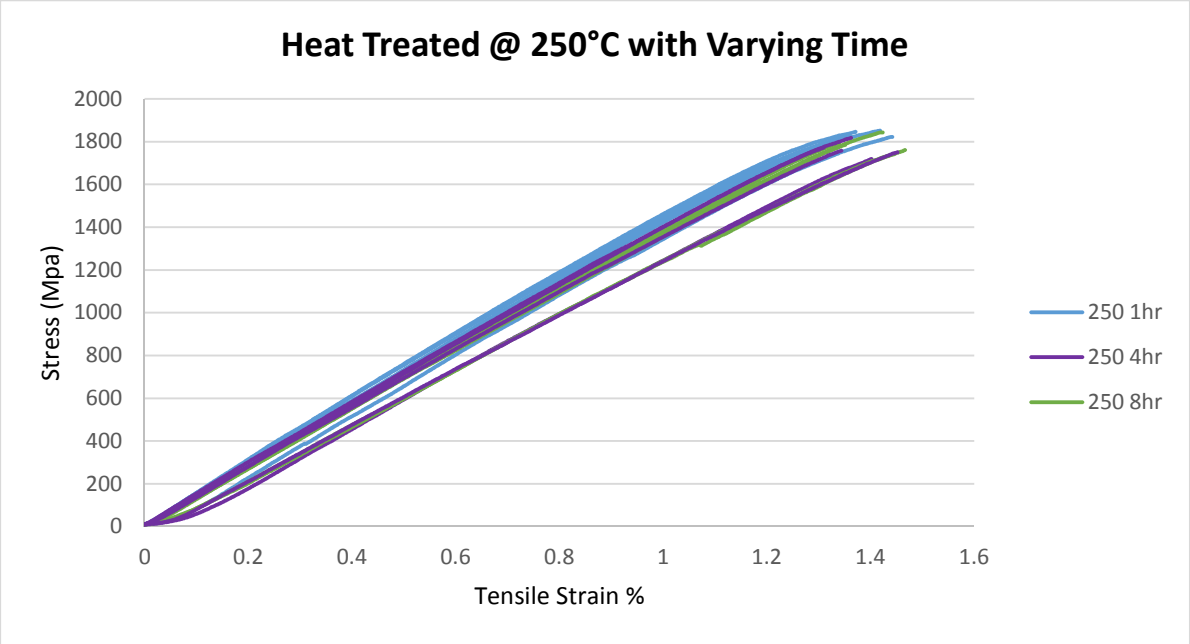

Figure 23: Heat treatments at 250°C with varying time showed little difference when compared to each other. All three times had a similar ductility and strength.

Heat treating at 400°C showed a decrease in strength from 250°C, with an ultimate tensile strength of 1705 MPa (Figure 24). This heat treatment decreased ductility, causing fracture at 1.30% strain. At the higher temperature the decrease in strength and ductility from 250°C may be due to competing mechanisms within the material causing the reduction strength and ductility.

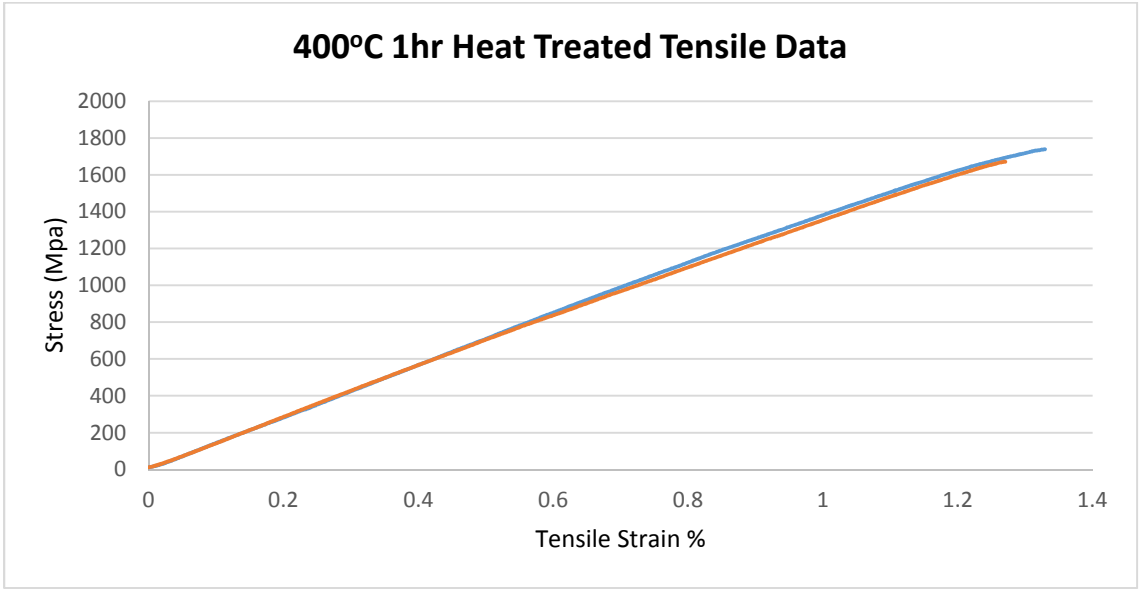

Figure 24: The 400°C wire showed a decrease in strength and a decrease in ductility. The curve shape of this treatment is also extremely linear in comparison to the cold worked wire.

Wire heat treated at 600°C deviated from the trend of the other heat treatments and caused the wire to have strengths and ductility similar to the SR wire (Figure 25). The wire had an average yield strength of 1231. The average percent elongation was 5.50%. The data appears to show that stress relief has occurred in the wire, which could be due to classic annealing, or some other mechanism within the wire.

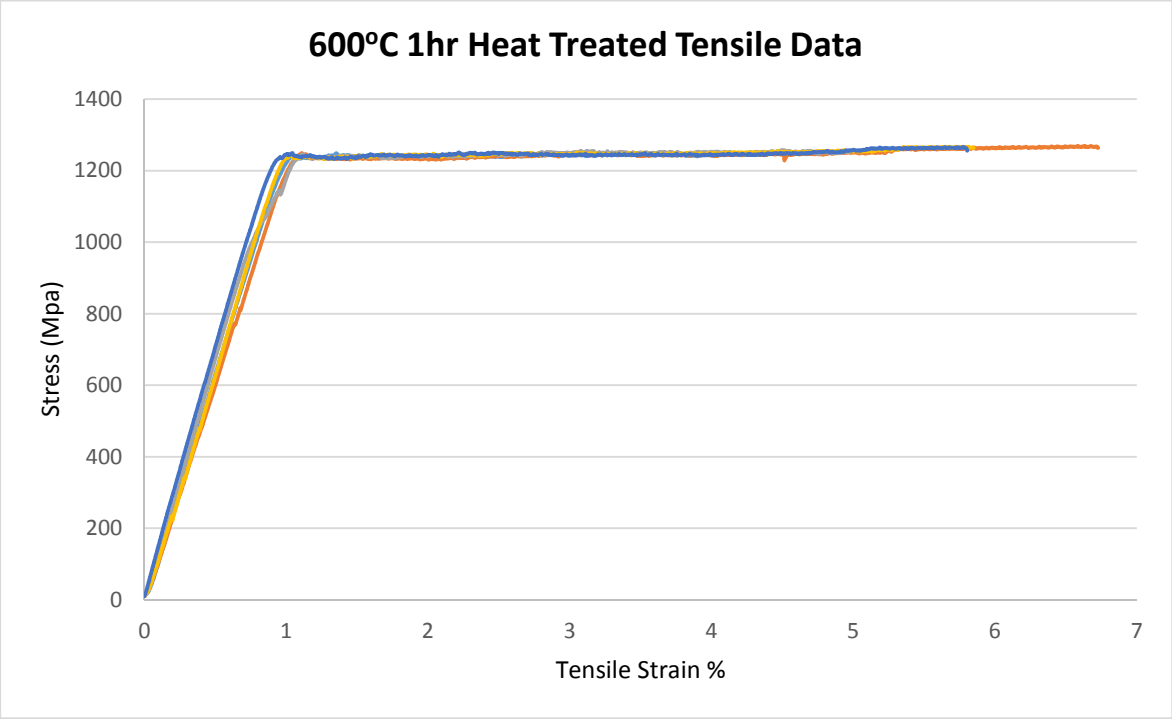

Figure 25: The 660°C heat treatment showed a return to the stress relieved state, and exhibited almost the exact same yield strength and ductility as the as-received stress relieved wire.

High strengths and low ductility were found in cold worked, 130°C, 250°C, and 400°C heat treated samples. Stress relieved and 600°C heat treated samples exhibited lower yield strengths and high ductility. Tensile tests results were averaged and placed onto one chart for comparison (Figure 26). Strength and ductility data is presented in Table III.

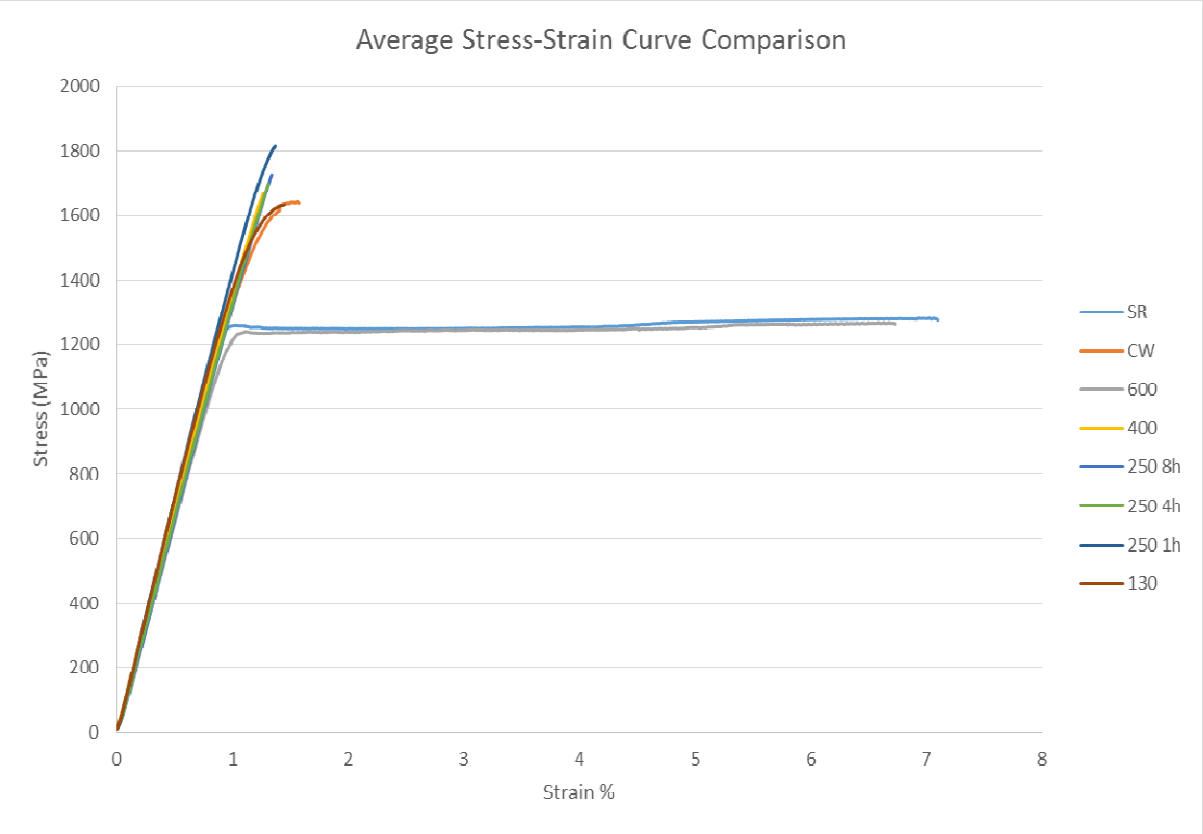

Figure 26: Average stress-strain behavior for each sample type. The graph shows the significant change in properties caused by differing heat treatment temperatures.

Table III: Average Mechanical Properties of Heat Treated and As-received Pt/Ni Wire

Sample	Yield Strength (MPa)	Strain at Fracture (%)
Stress Relieved	1251	6.89
Cold Worked	1600	1.43
130°C 1hr	1587	1.40
250°C 1hr	1829*	1.39
250°C 4hr	1763*	1.37
250°C 8hr	1784*	1.41
400°C 1hr	1705*	1.30
600°C 1hr	1231	5.50

*UTS instead of 0.2% offset YS

X-ray Diffraction

X-ray diffraction was done on the stress relieved, cold worked, and 250°C heat treated wire to look for ordering in the crystal structure. Scans of the three wire types tested all showed the (111), (200), (220), (311), and (222) fundamental reflections. Some reflections appeared smaller than expected and the signal-to-noise ratio was not ideal for the stress relieved and cold worked scans. Full scans and high resolution scans of superlattice sites indicated no signs of reflections for all wire types.

The X-ray diffraction of the stress relieved wire showed an adequate signal-to-noise ratio, but the noise level was not ideal (Figure 27). The (111) peak was fairly small, but the other fundamental reflections showed up with a good signal. There were no signs of superlattice reflections in the expected locations. The high resolution scans of each superlattice location showed no consistent deviation from the noise level.

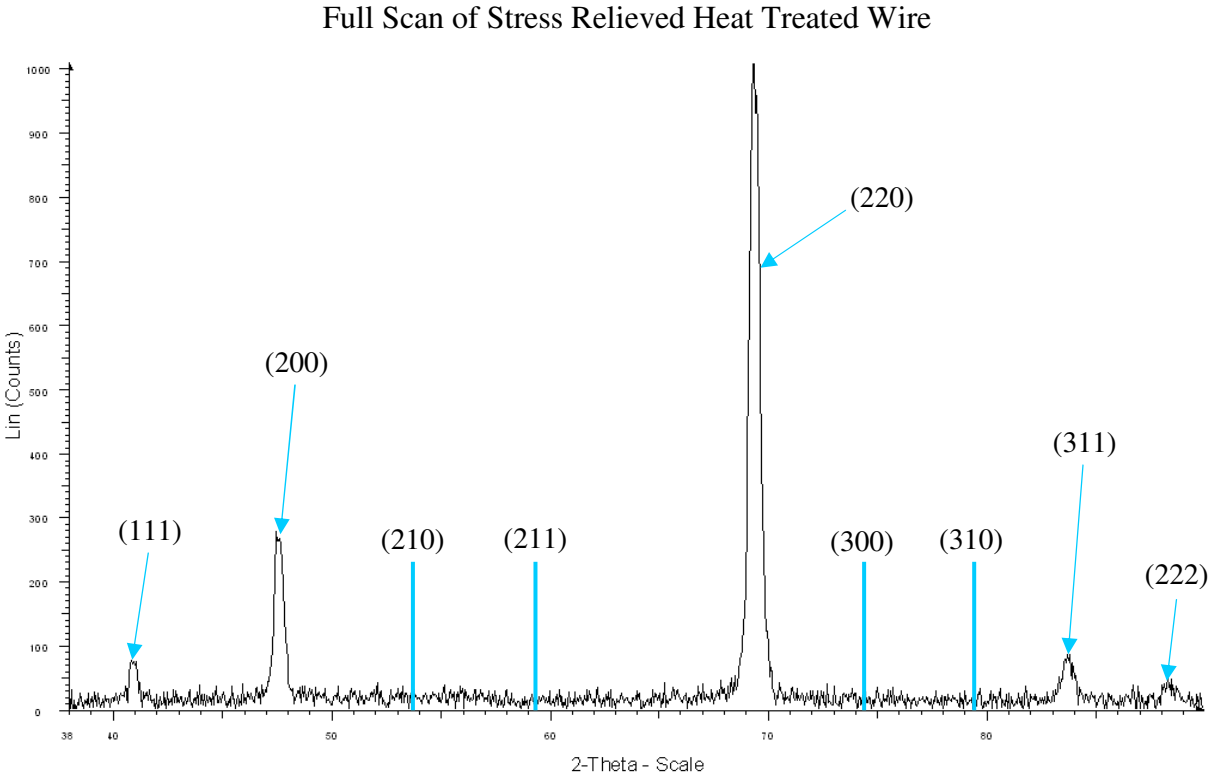

Figure 27: X-ray diffraction pattern of Stress Relieved wire from 38 to 90 2θ. Superlattice reflections are absent and are indicated by the blue lines. The (111) reflection is smaller than expected due to microstructure texture.

Diffraction analysis of the cold worked wire had worse signal-to-noise ratio than the stress relieved wire (Figure 28). This meant that some fundamental peaks, like the (111), were even harder to see. The (311) and (222) were also broad and barely stood above the noise. The noise levels in the cold worked scan did not show any superlattice reflections. High resolution scans of specific superlattice sites showed no indications of peaks.

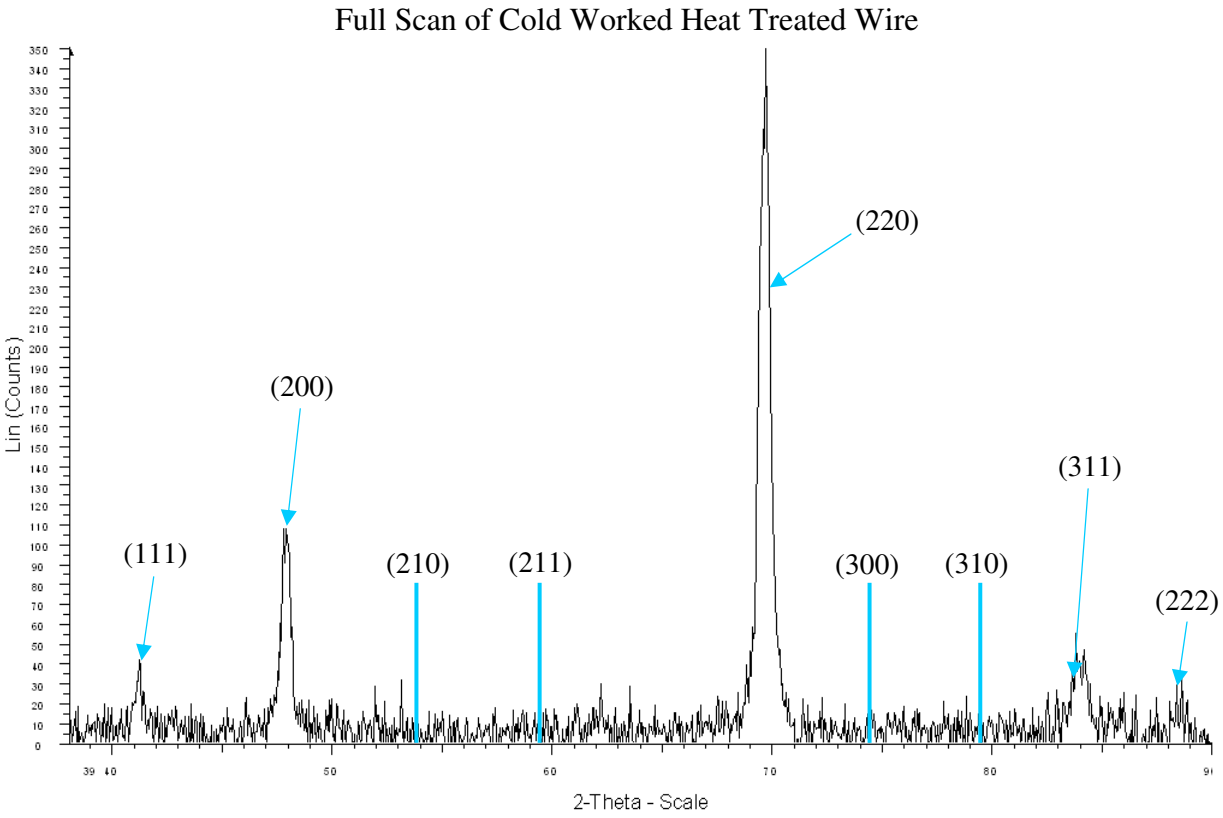

Figure 28: Cold worked wire diffraction pattern from 38 to 90 2θ. The signal-to-noise ratio was poor, due to difficulties with sample preparation. Superlattice reflection locations are shown by the blue lines.

The 250°C X-ray analysis of the wire gave good reflections from all the fundamental peaks, including the (111) peak (Figure 29). There was also a low noise level, which allowed for better resolution peaks. There were still no signs of superlattice reflections in this scan, even with the low noise level. High resolution scans of the superlattice sites were unsuccessful in finding any peaks.

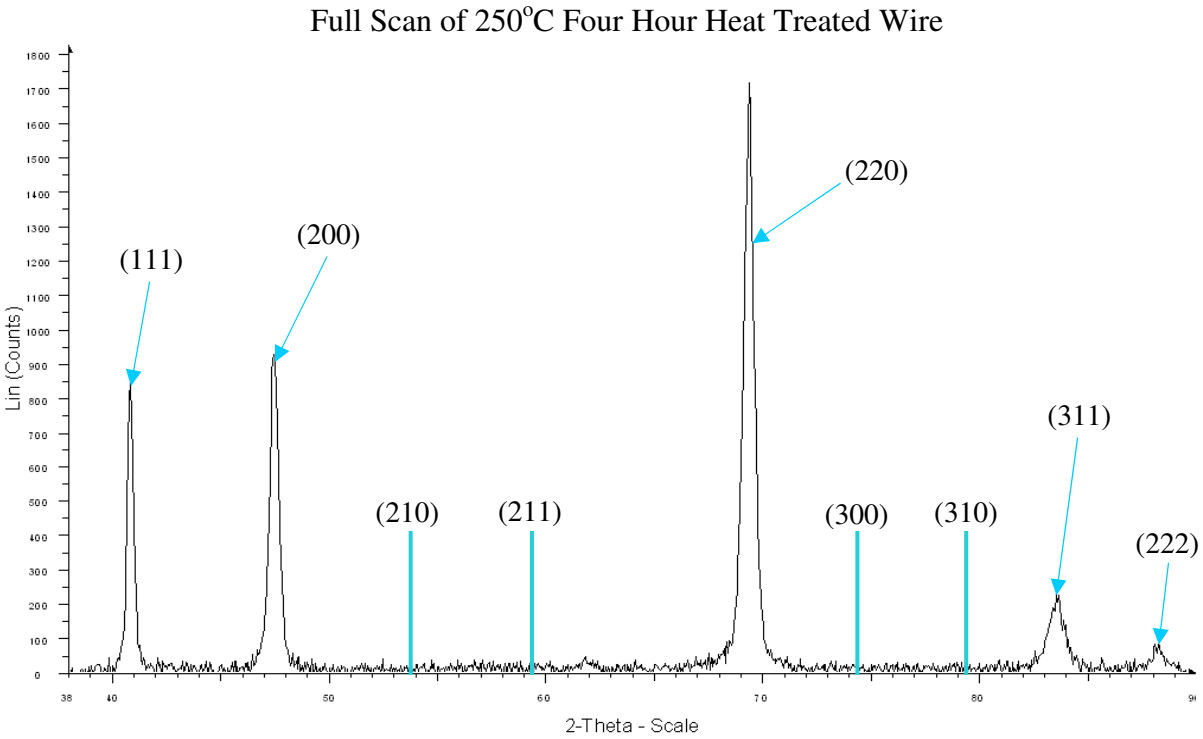

Figure 29: Diffraction pattern from 38 to 90 2θ of a 250°C four hour heat treated wire. Calculated superlattice reflection locations are indicated by blue lines. This scan represents the best signal-to-noise ratio achieved.

The height of the (111) peak was affected by heat treatments. A quantifiable comparison can be made by finding the (220) to (111) peak height ratio. The approximate value for the 250°C heat treated wire peak ratio is 2:1. This is significantly less than the same ratio for stress relieved and cold worked wire which are 13:1 and 8:1 respectively. This indicates a clear difference between the heat treated, cold worked, and stress relieved wire.

Discussion

Heat treatments on the wire had a clear effect on the mechanical properties. The temperatures were chosen in and around the ideal ordering range indicated by the CALPHAD phase diagram. The results of the tensile tests indicate that there is strengthening occurring in the region, however, it is unclear if this is due to ordering or another mechanism. The heat treatment outside of the ordered region at 600°C showed a completely different mechanical behavior than those within the region. The increased ductility, and lower yield strength in the 600°C sample compared to the other heat treatments, gives evidence for the idea of ordering within the wire, at

the ideal temperatures. However X-ray diffraction was not able to find any superlattice reflections within the wire, meaning that ordering may not be the mechanism of strengthening. It might also mean that XRD could not detect order due to the fine diameter and texture of the wire. Strain aging within the wire could also cause an increase in strength seen. The drop off in strength and return to the lower yield, highly ductile state is attributed to the annealing of the structure.

The 130^{o}C heat treatment had yield strength, ductility and a curve shape similar to the CW wire samples, from which it was heat treated. This indicates that the low temperature treatment had little metallurgical effect on the wire. Both ordering and strain aging are diffusion based processes. High amounts of diffusion are unlikely to occur at 130^{o}C in this alloy system. The yield strength and curve shape of both the 130^{o}C and CW samples likely comes from high amounts of cold work.

The 250^{o}C heat treatment shows the highest strengths of all treatments. The various times used at this temperature had little effect on the mechanical behavior of the wire. This indicates that the mechanism strengthening the wire is a fairly fast process with little time dependence. 250^{o}C is in the center of the ordered phase range and the strength may be a result of ordering. The CALPHAD modeled phase diagram suggests that ordering should be found in this region but high strength alone does not confirm this hypothesis. The heat treatment may have caused other temperature activated mechanisms, such as strain aging.

Heat treating the wire at 250^{o}C for multiple temperatures showed little change in the yield strength or the ductility of the wire. The only change that was seen was a decrease in strength. This indicates that the strengthening from the heat treatments occurs within the first hour. The short time dependency could be due to the mechanism itself, or the small sample geometry. Both mechanisms are diffusion based and the small sample size would allow the temperature of the entire sample to change rapidly. Ordering which could be occurring, would show an increase in strength as the alloy orders. This strength would reach a peak when there is an ideal amount of antiphase boundaries, then begin to drop off as the anti-phase domains grow within the grains. A similar result can be seen in the wires tested, with the one hour heat treatment having the highest

tensile strength, and the four and eight hour treatments having a lower strength. More samples would need to be tested in order to prove a statistical difference each of the heat treatment times. Wire of this diameter could be susceptible to drastic changes in strength, due to even the smallest defects on the wires surface. The scatter seen in these tests could be a result of this phenomena, so a larger sample size should be run to eliminate this variable from affecting the results. The decrease in strength seen in the time variation treatments does not support the hypothesized strain aging. Strain aging should cause a continuous increase in yield strength over time as more dislocations become pinned, which would increase strength. The decrease in strength indicates that ordering could be the method of strengthening, not strain aging.

The 400^{o}C heat treatments show a small decrease in strength from the strongest samples as well as lower ductility. The curves' linear shape indicates a brittle failure with little to no yielding. 400^{o}C is near the upper limit of the ordered range and maintains the high strength and low ductility experienced by other heat treatments in this region. The lower strength of this heat treatment may indicate some stress relieving. Annealing of a highly cold worked structure can occur at lower temperatures than expected due to the increased strain energy available within the material.

The highest heat treatment of 600^{o}C showed a significant change in strength and ductility. The yield strength of 1231 MPa was similar to the stress relieved. Additionally, the ductility of the wire was increased by 6%. The deviation from the behavior of other heat treated wire shows that at high temperatures the structure of the wire is changed. 600^{o}C is outside of the theoretical ordered region. If the wire becomes ordered at lower temperatures and disordered at 600^{o}C the decrease in strength can be attributed to the recrystallization of the structure at elevated temperatures. This annealing would decrease the strength for both an ordered or strain aged alloy.

The stress relieved wires that Abbott uses show significant ductility and a relatively low yield strength in comparison to the heat treated wires. This is due to the stress relieving process that they use on the wires, which is similar to the 600^{o}C heat treatment. The cold worked wire appears to draw its strength from the large amounts of dislocations in the structure. The role of

ordering or strain aging within these two wires is not known. If ordering is present, it may be present in the cold worked wire but would not be found in the stress relieved. Strain aging might be present within the stress relieved or cold worked wire.

Heat treating causes a strengthening within the alloy, which increases as temperature increases to a peak around 250°C and then decreases as temperature increases after this point. The strengthening also does not increase with time, after peaking at less than or equal to an hour. These phenomena seem to indicate ordering within the alloy due to the nature of the mechanism, and the ideal ordering range on the phase diagram (Figure 30). This could also be explained by strain aging with Cottrell atmospheres, and an annealing process within the wire.

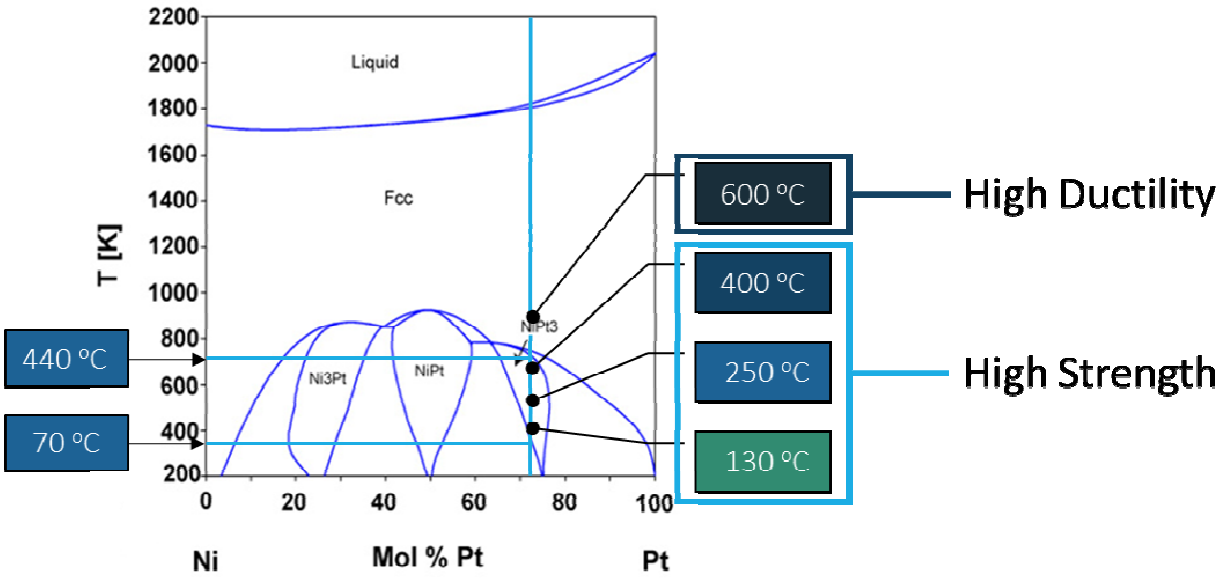

Figure 30: Heat treatment temperatures shown with their locations on the computer modeled phase diagram. The temperatures within the ordered region showed high strength and the temperature outside showed low strength with high ductility.

A one-way ANOVA (unstacked) was performed on the yield strengths to find the statistical significance of the tensile tests. A Tukey comparison test was also performed on the data to show the grouping of each test (Figure 31). This analysis showed with 99% confidence that the stress relieved wire and the 600°C heat treatment were in the same grouping. This means that the 600°C heat treatment was able to achieve the same strength as the stress relieved wire. It also showed with 99% confidence that the cold worked wire and the 130°C heat treatment were the same strength. Proving that this heat treatment did nothing to affect the strength. In addition, the

Tukey grouping showed that the 250°C for one hour and the 250°C for eight hours were the same. The 250°C eight hour was in the same grouping as the four hour and the 400°C heat treatments.

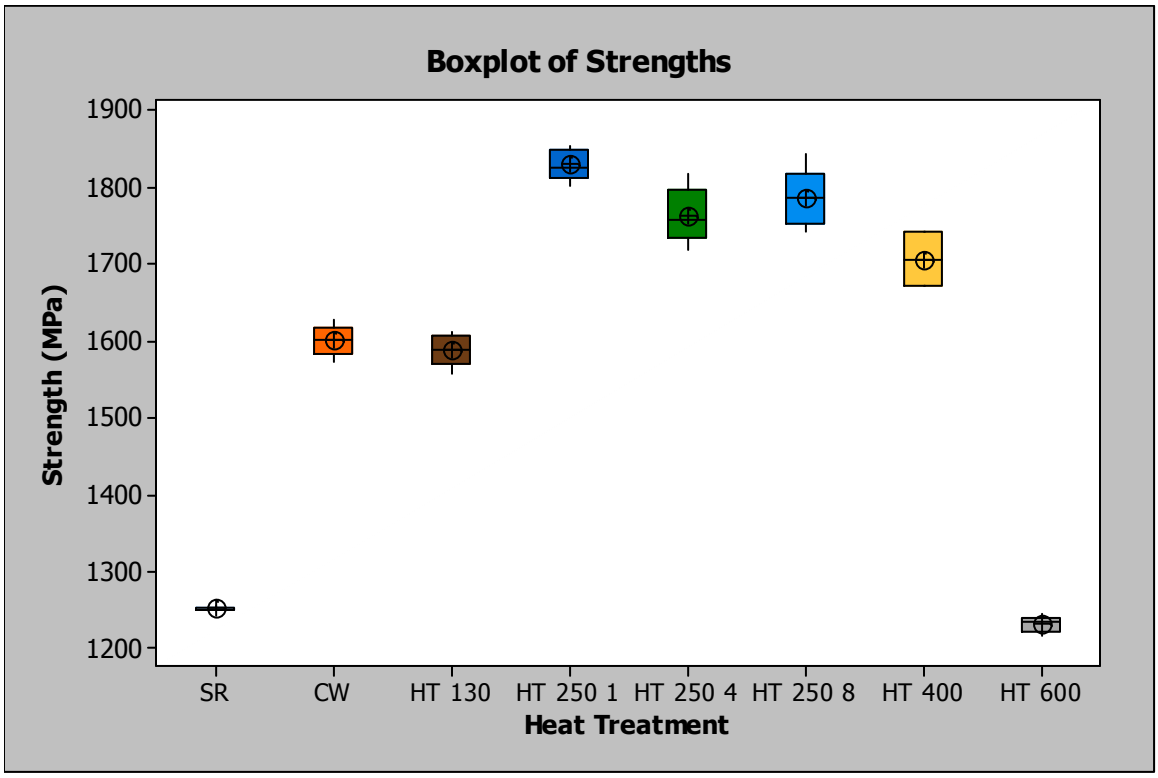

Figure 31: The boxplot of strength distributions for each sample type. Statistical overlap can be seen in several of the samples. However, a clear difference is seen in some of the heat treated samples.

X-ray analysis of the stress relieved, cold worked, and 250°C heat treated wires did not show ordering. Cold working the wire during wire drawing produces a grain structure that has a preferred crystallographic orientation, or elongation of grains along preferred slip planes and directions. The high amounts of cold work in the wire could obscure the superlattice reflections. When the wire contains large amounts of grains with preferred crystallographic orientation, texture is observed in X-ray diffraction. The texture of the wire can cause the decrease in the reflection of certain crystallographic planes.[13] In the stress relieved and cold worked wire tested, the texture effect caused the (111) plane to be noticeably smaller than expected. In future studies, an X-ray diffractometer with a sample stage that has 2 free axes of rotation is recommended. This would decrease the texture effect, by being able to view the aligned slip planes from multiple angles, increasing the signal they exhibit.

The fine diameter of the wire samples caused additional difficulties with X-ray diffraction testing. Preparation of samples with fine wire for X-ray diffraction causes a non-ideal signal-to-noise ratio due to non-ideal diffraction circle coverage. The profile of the wire causes peaks to broaden and in general return less counts. While superlattice reflections were not found, it is possible that a combination of issues with sample preparation and geometry caused their absence and not the lack of ordering.

The lower (220) to (111) peak ratio of 2:1 in the 250^{o}C XRD scan, compared to the much higher peak ratios of the other two wire types can be explained by one of two things (Figure 27, 28, 29). The sample was heat treated, and could have recrystallized a significant amount compared to the other wires. In this case, the stress relieved wire would also show recrystallization and the appearance of the (111) peak. However, the stress relieved wire is heat treated while still under tension which may cause alteration to the crystallographic orientation. This could cause the reemergence of the peak that was seen in the 250^{o}C scan and the peak's absence in the other scans. Another probable explanation is due to sample preparation of the wire. The cold worked and stress relieved wires both were prepared by bundling, in parallel, one long wire which was taped at both ends to a slide. This allowed some gaps between the slide and the wire and a rough surface, which is not ideal for X-ray diffraction. The 250^{o}C heat treated wire had a much more meticulous sample preparation, where 50 wires were laid side by side onto double sided tape to form a much flatter surface. This could cause a difference in the diffraction pattern as seen by the better signal-to-noise ratio and higher peaks in the 250^{o}C sample.

The theory that strain aging caused by Cottrell atmospheres requires further investigation with advanced testing methods. TEM analysis of dislocation sites for atmospheres could indicate their presence. However, sample preparation for TEM using fine wire poses challenges and is beyond the scope of this project.

Overall, strength was increased at moderate temperatures within the expected Pt_3Ni region, and ductility was increased at temperatures above this region with a sacrifice to strength. A strengthening mechanism is activated by the heat treatment. The tensile results alone suggest that

ordering increases strength. However, X-ray diffraction does not indicate the presence of superlattices caused by ordering. While it is possible that ordering is present but not detectable in the wire, it is recommended that other mechanisms, including strain aging, be evaluated for their presence in the wire.

Conclusions

Platinum-Nickel wire used by Abbott Vascular shows an abrupt transition from elastic to plastic behavior as well as high ductility in the stress relieved state. The cold worked state has higher strength at 1600 MPa. The lowest heat treatment of 130^{o}C to the cold worked wire showed little metallurgical effect. Heat treatments of 250^{o}C and 400^{o}C cause the wire to increase in strength from the cold worked state. The highest strength achieved was 1829 MPa with the 250^{o}C treatment for one hour. 600^{o}C heat treatments cause the wire to behave similarly to the stress relieved samples with lower strength and high ductility.

Heat treatments within the theoretical ordered region increased the strength of the wire and the 600^{o}C treatment, outside of the ordered region, showed lower strength. This indicates that ordering causes the system to strengthen. However, no evidence of ordering was found using X-ray diffraction. While this does not necessarily disprove the ordering hypothesis, the alternative theory of Cottrell atmospheres causing strain aging must be considered as a possible strengthening mechanism. Further analysis of this system is required to prove which strengthening mechanism is present in the platinum/nickel wire.

References

1. Abbott Laboratories. Form 10 K/A. December 31 2012. SEC Archives Online. Web. 29 Jan. 2015.
2. Abbott Laboratories. 2013 Annual Report. Providence, RI. Abbott Laboratories. 2014
3. "What Are Medical Guidewires and Their Uses?" *Shannon MicroCoil*. N.p., n.d. Web. 05 Dec. 2014.
4. "Guidewire Technologies, Inc." Guidewire Technologies, Inc. N.p., n.d. Web. 30 Jan. 2015.
5. Goodney, Phillip P., Adam W. Beck, Jan Nagle, Gillbert H. Welch, and Robert M. Zowlak. "National Trends in Lower Extremity Bypass Surgery, Endovascular Interventions, and Major Amputations." Journal of Vascular Surgery 50.1 (2009): 54-60. Science Direct. Web. 12 Nov. 2014. <http://www.sciencedirect.com/science/article/pii/S0741521409000548>.
6. Simpson, John. "Property Differences in 90Pt/10Ni vs. 90Pd/10Re Wire Used in Tip Coils." Lecture.
7. Reza Abbaschian, Lara Abbaschian, Robert E. Reed-Hill. Physical Metallurgical Principles 4th Edition. Cengage Learning.
8. Intermediate Phases. Approved by the ASM Handbook Committee for addition to the ASM Handbooks Online, *Alloy Phase Diagrams*, Volume 3, ASM International, 2012.
9. J. Regina, Ordered Structures, Metallography and Microstructures, Vol 9, ASM Handbook, ASM International, 2004, p. 144–147
10. A.E. Vidoz & L. M. Brown (1962): On work-hardening in ordered alloys, Philosophical Magazine, 7:79, 1167-1175
11. P. Nash and M.F. Singleton, Ni-Pt (Nickel-Platinum), Phase Diagrams of Binary Nickel P. Nash, Ed., ASM International, Materials Park, OH, 1991, p 261-264
12. X.G. Lu, B. Sundman, and J. Ågren. Thermodynamic Assessment of the Ni-Pt and Al-Ni-Pt Systems. Calphad. 2009. 33. p 450-456
13. Suryanarayana, C., and M. Grant. Norton. X-ray Diffraction: A Practical Approach. New York: Plenum, 1998. Print.
14. Tawancy, H. M. "Long-range Ordering Behaviour and Mechanical Properties of Ni-Mo-based Alloys." Journal of Materials Science 30.2 (1995): 522-37

15. Thompson, Robert Wayne, "The effect of nitrogen on the strain aging and brittle-ductile transition of vanadium" (1964). Retrospective Theses and Dissertations. Paper 3826.
16. Cahn, R. W., and P. Haasen. "15.4.1.2 Segregation to Dislocations." Physical Metallurgy. 5th ed. Vol. 1. Amsterdam: North-Holland Physics Pub., 1983. 1515. Print.

Appendix

Tensile Test Data

Stress Relieved: 5 samples, average σ_y = 1251 MPa, average ductility 6.89%

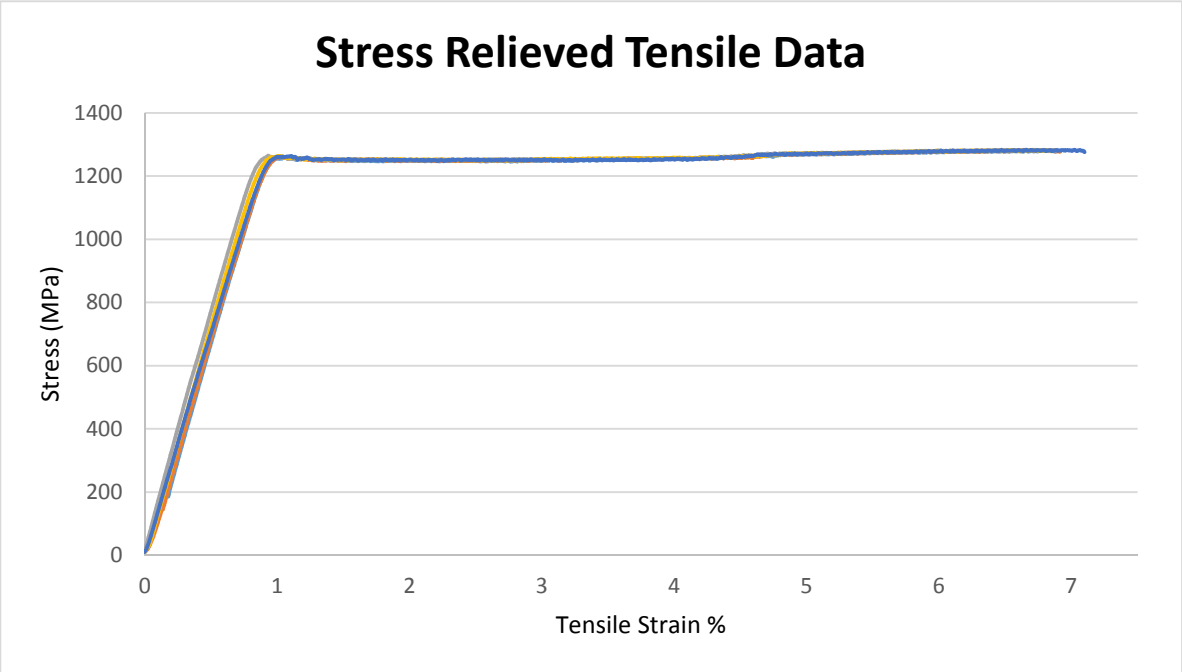

Cold Worked: 5 samples, average σ_y = 1600 MPa, average ductility 1.43%

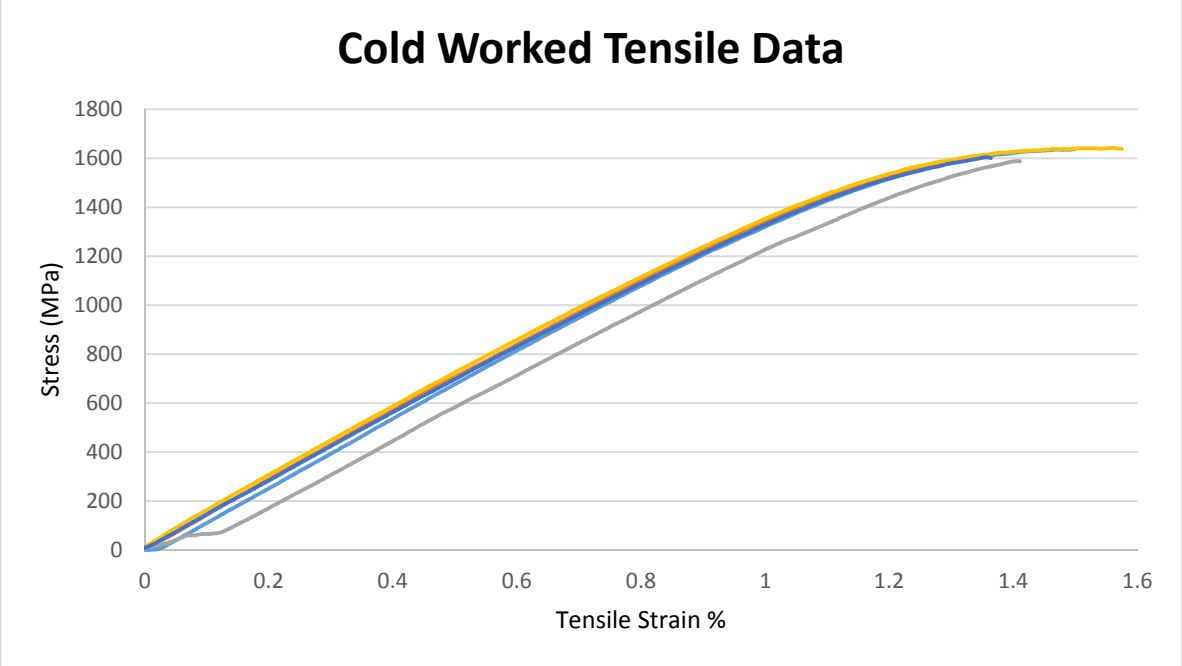

130°C 1hr heat treated: 5 samples, average σ_y = 1587 MPa, average ductility 1.40%

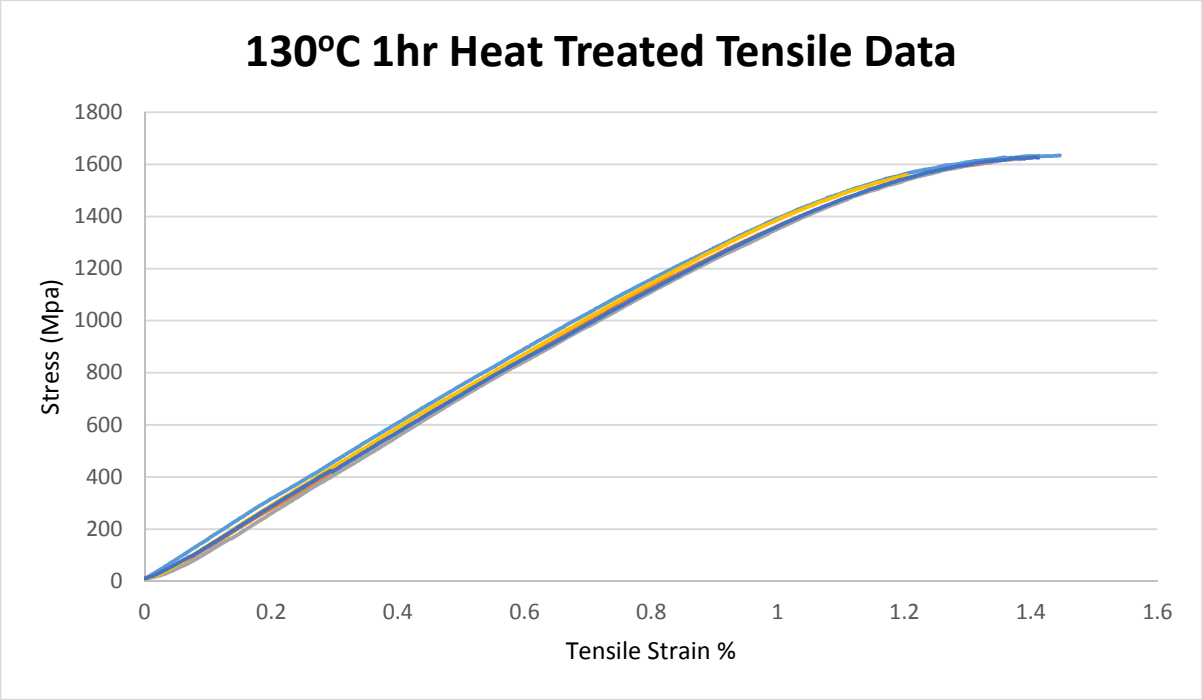

250°C 1hr heat treated: 5 samples, average σ_y = 1829 MPa, average ductility 1.39%

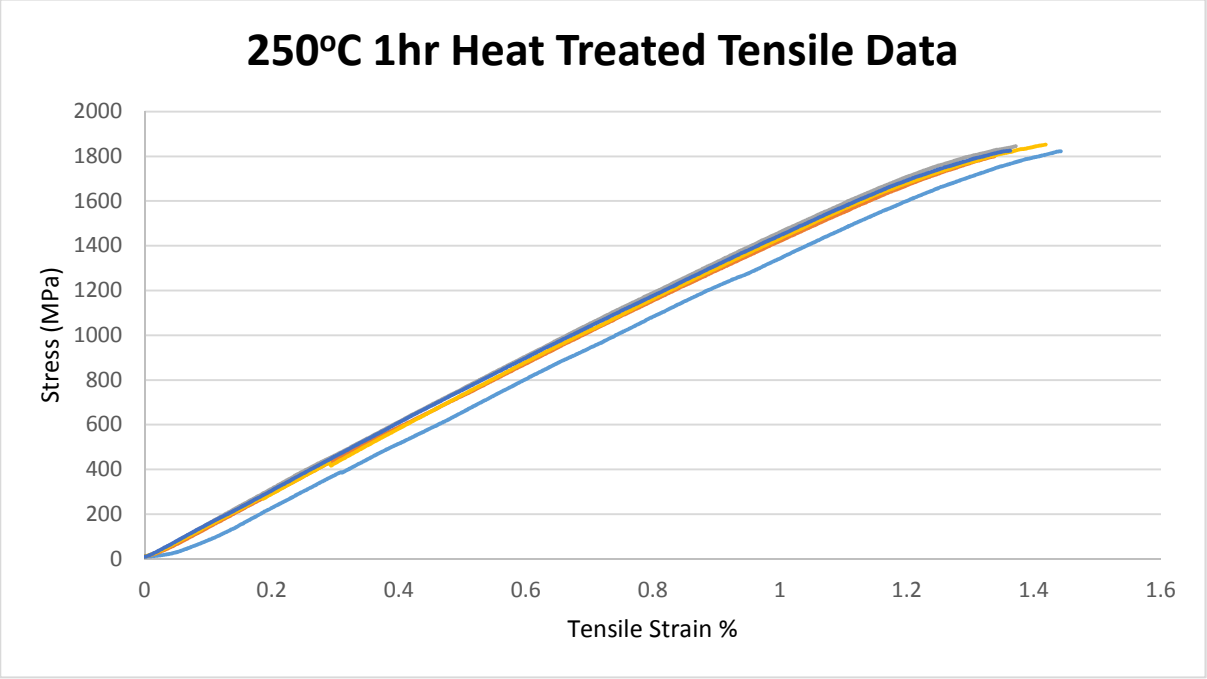

250°C 4hr heat treated: 5 samples, average σ_y = 1763 MPa, average ductility 1.37%

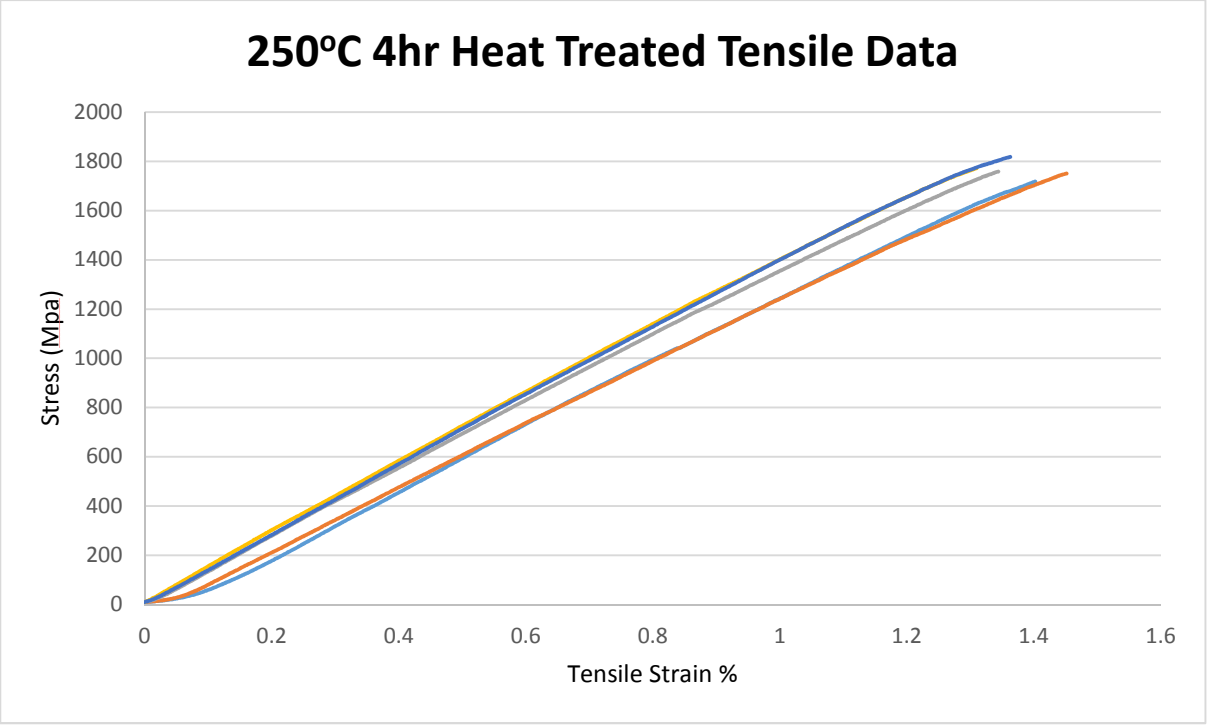

250°C 8hr heat treated: 5 samples, average σ_y = 1784 MPa, average ductility 1.41%

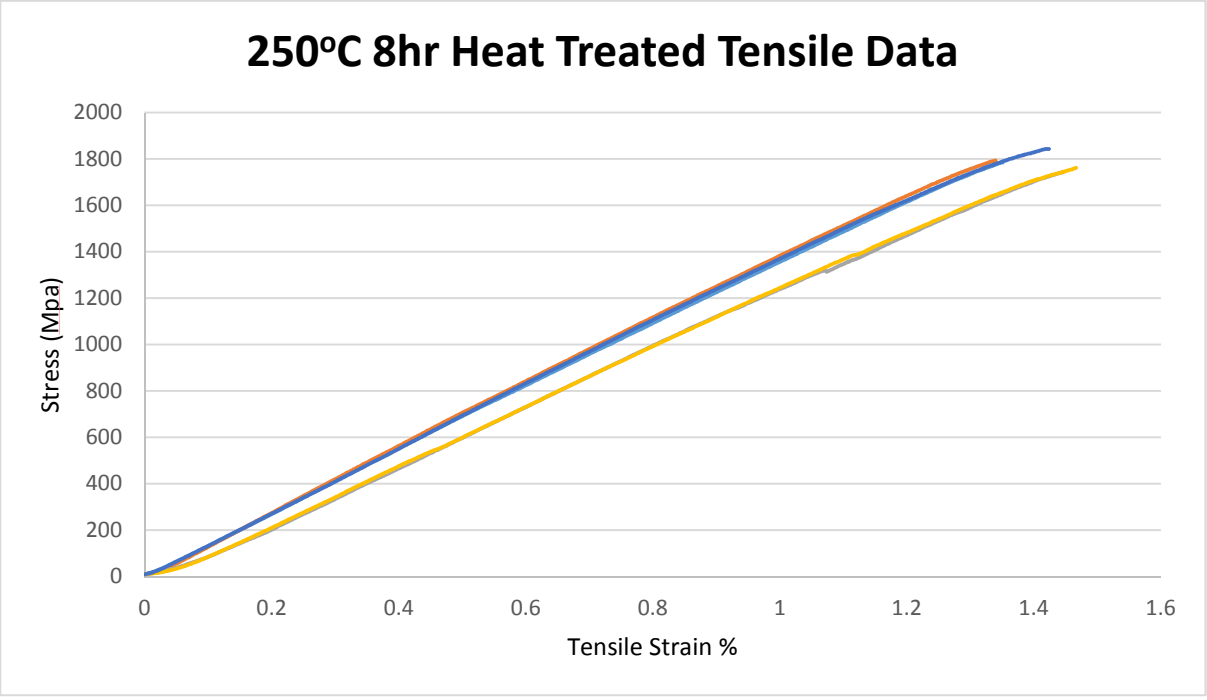

400°C 1hr heat treated: 2 samples, average σ_y = 1784 MPa, average ductility 1.30%

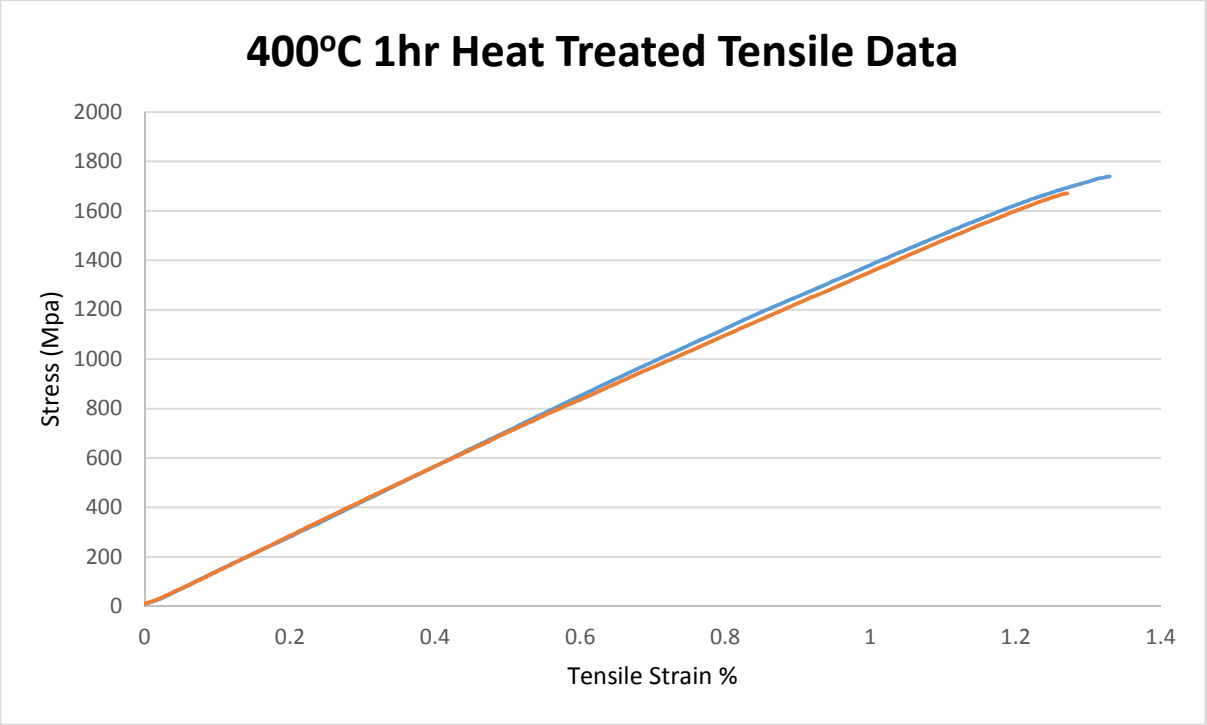

600°C 1hr heat treated: 2 samples, average σ_y = 1231 MPa, average ductility 5.50%

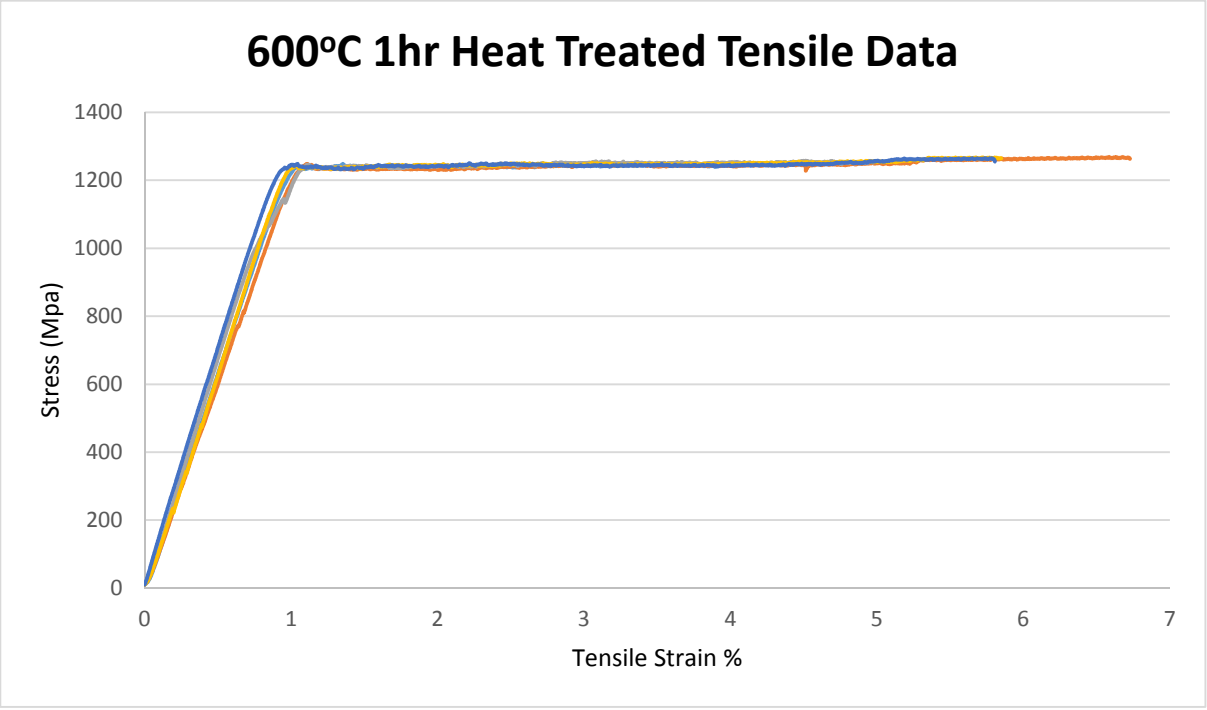

X-ray Diffraction Data

Stress Relieved Wire Full Scan

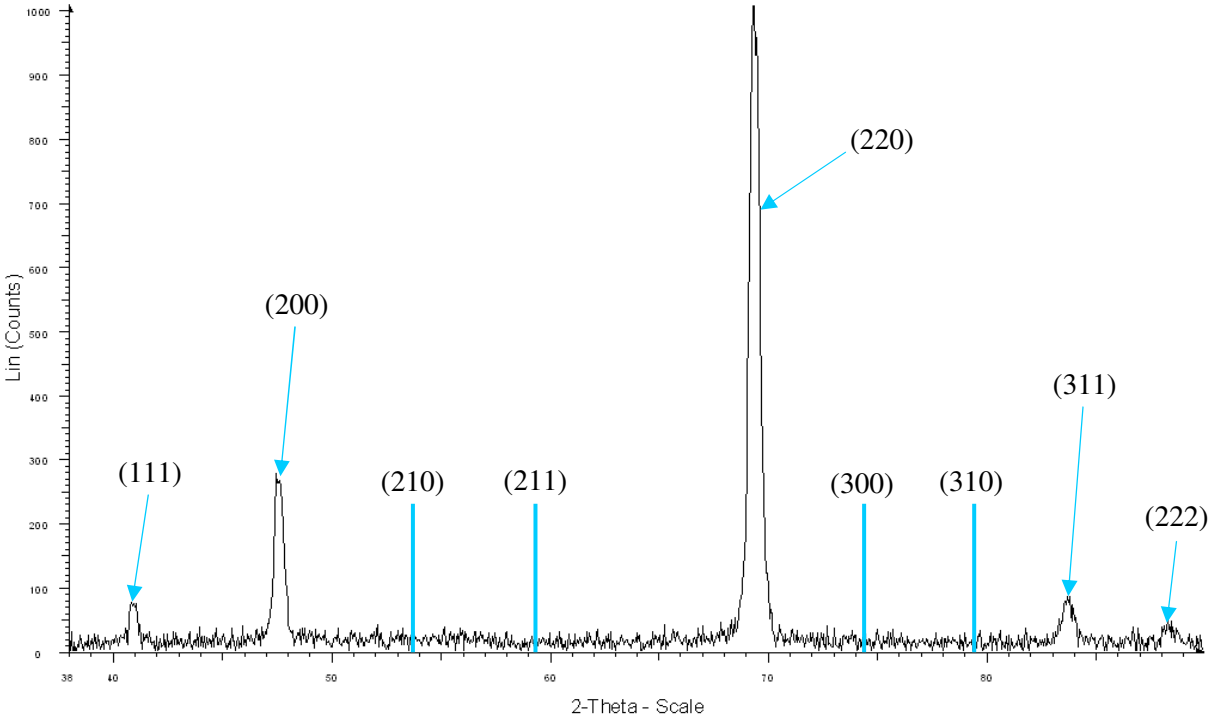

Cold Worked Wire Full Scan

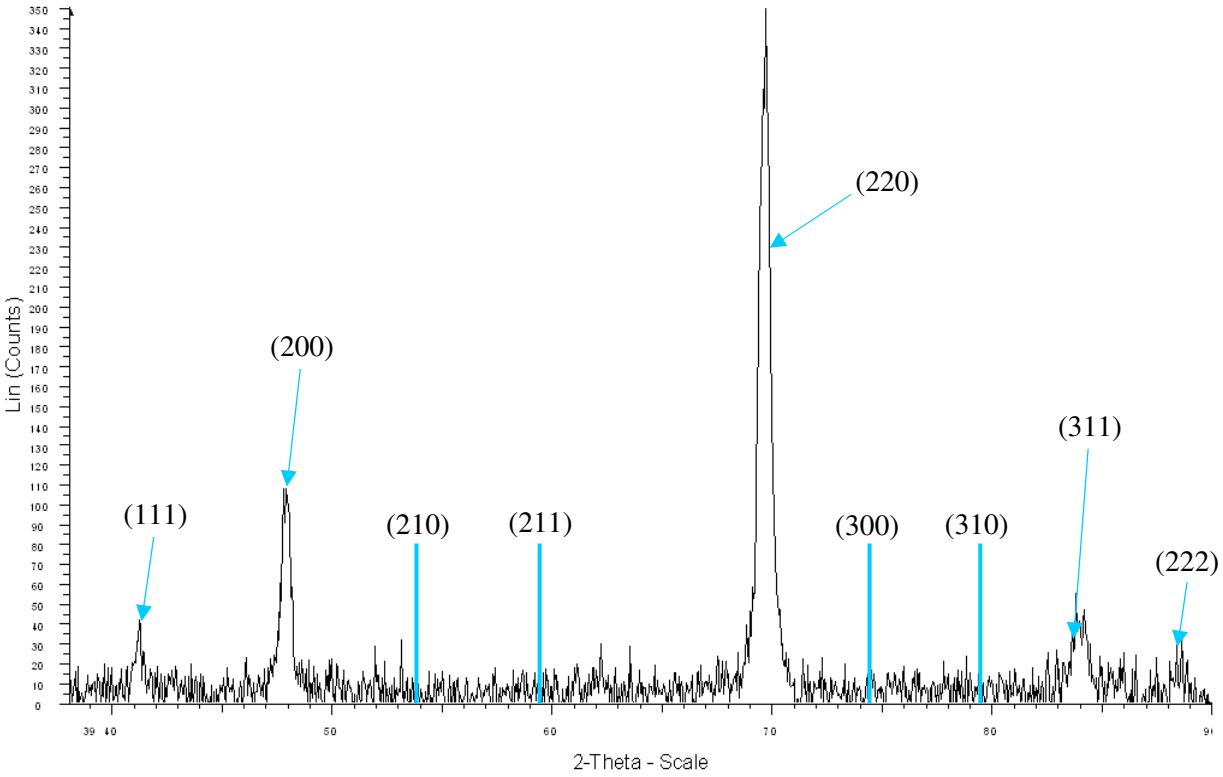

250°C 1hr Heat Treated Wire Full Scan

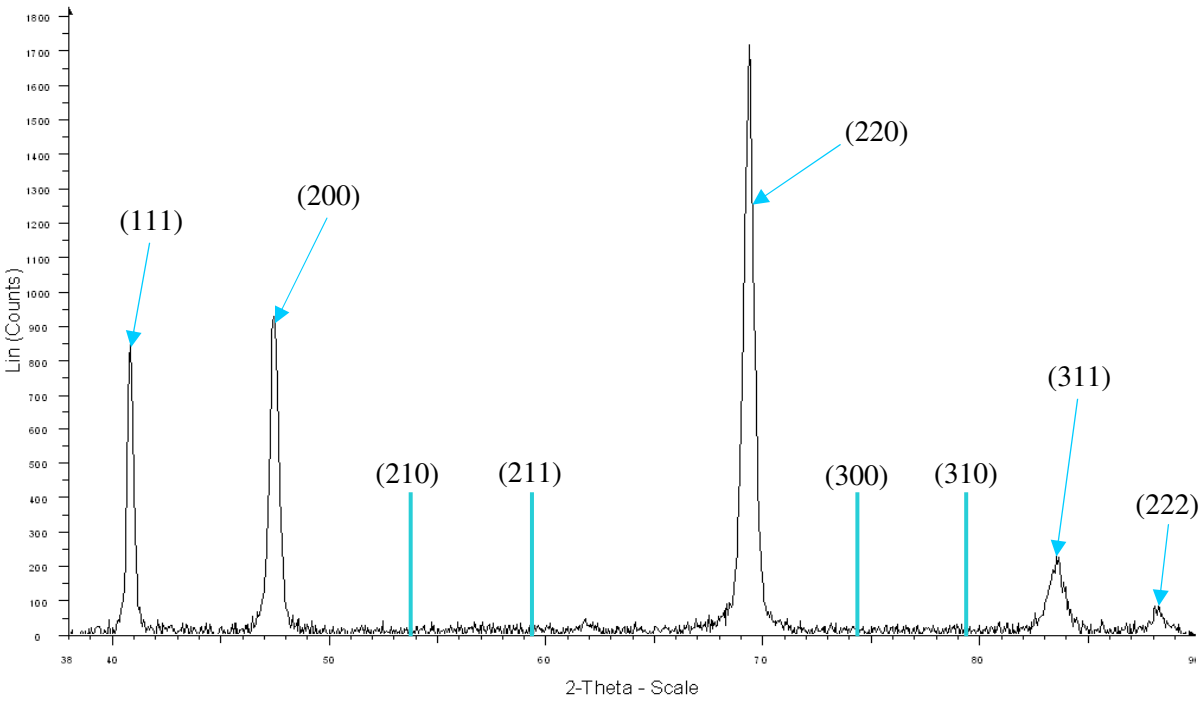

Minitab output for one-way ANOVA Testing

```
Grouping Information Using Tukey Method

          N     Mean  Grouping
HT 250 1  5  1828.96  A
HT 250 8  5  1784.14  A B
HT 250 4  5  1763.12    B
HT 400    2  1705.00    B
CW        5  1600.20      C
HT 130    5  1587.20      C
SR        5  1250.92        D
HT 600    5  1230.62        D

Means that do not share a letter are significantly different.


Tukey 99% Simultaneous Confidence Intervals
All Pairwise Comparisons

Individual confidence level = 99.95%




SR subtracted from:
```

```
           Lower  Center   Upper  ---------+---------+---------+---------+
CW        285.69  349.28  412.87                            (-*-)
HT 130    272.69  336.28  399.87                            (-*)
HT 250 1  514.45  578.04  641.63                                   (-*)
HT 250 4  448.61  512.20  575.79                                 (-*)
HT 250 8  469.63  533.22  596.81                                 (-*-)
HT 400    369.96  454.08  538.20                               (-*-)
HT 600    -83.89  -20.30   43.29                    (*-)
                                  ---------+---------+---------+---------+
                                        -350         0       350       700
```

CW subtracted from:

```
            Lower   Center    Upper  ---------+---------+---------+---------+
HT 130     -76.59   -13.00    50.59                   (-*)
HT 250 1   165.17   228.76   292.35                         (-*)
HT 250 4    99.33   162.92   226.51                       (-*)
HT 250 8   120.35   183.94   247.53                       (-*-)
HT 400      20.68   104.80   188.92                     (-*-)
HT 600    -433.17  -369.58  -305.99          (*-)
                                  ---------+---------+---------+---------+
                                        -350         0       350       700
```

HT 130 subtracted from:

```
            Lower   Center    Upper  ---------+---------+---------+---------+
HT 250 1   178.17   241.76   305.35                         (-*-)
HT 250 4   112.33   175.92   239.51                       (-*-)
HT 250 8   133.35   196.94   260.53                        (-*)
HT 400      33.68   117.80   201.92                     (-*--)
HT 600    -420.17  -356.58  -292.99          (-*-)
                                  ---------+---------+---------+---------+
                                        -350         0       350       700
```

HT 250 1 subtracted from:

```
            Lower   Center    Upper  ---------+---------+---------+---------+
HT 250 4  -129.43   -65.84    -2.25                 (-*-)
HT 250 8  -108.41   -44.82    18.77                  (-*-)
HT 400    -208.08  -123.96   -39.84               (-*--)
HT 600    -661.93  -598.34  -534.75  (-*-)
                                  ---------+---------+---------+---------+
                                        -350         0       350       700
```

HT 250 4 subtracted from:

```
            Lower   Center    Upper  ---------+---------+---------+---------+
HT 250 8   -42.57    21.02    84.61                    (-*)
HT 400    -142.24   -58.12    26.00                 (-*--)
HT 600    -596.09  -532.50  -468.91    (-*-)
                                  ---------+---------+---------+---------+
                                        -350         0       350       700
```

HT 250 8 subtracted from:

```
          Lower   Center    Upper  ---------+---------+---------+---------+
HT 400  -163.26   -79.14     4.98               (--*-)
HT 600  -617.11  -553.52  -489.93   (-*-)
                                   ---------+---------+---------+---------+
                                         -350         0       350       700
```

HT 400 subtracted from:

```
          Lower   Center    Upper  ---------+---------+---------+---------+
HT 600  -558.50  -474.38  -390.26     (-*--)
                                   ---------+---------+---------+---------+
                                         -350         0       350       700
```